

Supporting Information

Xiantao Hu,^{a†} Ram Datt,^{b†} Qiao He,^a Panagiota Kafourou,^a Harrison Ka Hin Lee,^{b,c} Andrew J. P. White,^a Wing Chung Tsoi,^{b*} and Martin Heeney^{a*}

¹Department of Chemistry and Centre for Processable Electronics, White City Campus, Imperial College London W12 0BZ, UK. E-mail: m.heeney@imperial.ac.uk

²SPECIFIC, Faculty of Science and Engineering, Bay Campus, Fabian Way, Swansea University SA1 8EN, UK. E-mail: w.c.tsoi@swansea.ac.uk

†These authors contributed equally to this work.

Materials:

Commercially available reagents were purchased and used without further purification unless otherwise stated. Malononitrile, 4,7-dibromo-5,6-difluorobenzo[c][1,2,5]thiadiazole, 4,6-dibromo-5-fluorobenzene[c][1,2,5]thiadiazol and 4,9-dihydro-s-indaceno[1,2-b:5,6-b']dithiophene were purchased from TCI Chemical and Sigma-Aldrich. PCE12, PM6, PM7, PTQ10 donor molecules were purchased from 1-Materials and applied without further purification. MoO₃ was purchased from STREM Chemicals UK LTD.

Measurements:

¹H NMR and ¹³C NMR spectra were recorded on Bruker AV-400 spectrometer using CDCl₃ as solvent at room temperature. Gas chromatography–mass spectrometry (GC-MS) was carried out on an Agilent GC 7890A and MS 5975C. Matrix-assisted laser desorption/ionization time-of-flight (MALDI-TOF) mass spectrometry was performed on a Bruker ultrafleXtreme MALDI-TOF analyzer. Computational details were presented as follows: Density functional theory calculations were performed using Gaussian G09 rev.d01 and GaussView 5.0.9 visualization software, using the B3LYP functional. Geometry optimizations were performed with full relaxation of all atoms in gas phase without solvent effects. And the octyl side chains were replaced by methyl ones for simplification. UV-vis spectra were recorded on a UV-1601 Shimadzu UV-vis spectrometer. Electrochemical measurements were carried out under nitrogen with a deoxygenated solution of tetra-n-butylammonium hexafluorophosphate (0.1 mol L⁻¹) in CH₃CN using a computer-controlled CHI660C electrochemical workstation, a platinum rod working electrode (Bioanalytical Systems Inc, 1.6 mm diameter) coated with samples, a platinum-wire auxiliary electrode, and Ag/AgCl as a reference electrode. Potentials were referenced to ferrocenium/ferrocene (FeCp^{2+/0}) couple by using ferrocene as an internal standard. Single-crystal X-ray Diffraction (XRD) was performed on Agilent Xcalibur 3 E. Crystals were grown as follows: about 4 mg solute dissolved in 0.5 ml dichloromethane was filtered before being put in a small vial sealed with a cap with a hole. This small vial was placed in a larger vial containing 2.5 ml cyclohexane. Then the outer container was closed. After

equilibration via vapour diffusion for one week, a yellow crystal suitable for analysis was formed.

Solar cells fabrication:

The fabricated device has inverted structure of glass/ITO/ZnO/active layer/MoO₃/Ag. The ITO substrates (15 Ω/sq, Lumtec Taiwan) were ultrasonically cleaned in a soap solution and deionized water (18 MΩ), followed by acetone (Fisher Scientific) and isopropyl alcohol (Fisher Scientific) for 10 minutes each. The dried ITO substrates were subjected to plasma treatment for 2.5 minutes. The zinc oxide (ZnO) precursor solution spin-coated at the speed of 4000 rpm, 40 s followed by thermal annealing at 150 °C for 10 minutes. It formed 35 nm ZnO film and act as electron transport layer. After cooling down, the substrates transferred into nitrogen filled glovebox. The active layer (PM6, FBTSCN-IDT, BTSCN-IDT) prepared in a 12 mg and 15 mg/ml anhydrous chloroform and chlorobenzene solvent, respectively, and at the donor-acceptor ratio of 1:2. The prepared active layer blend coated on top of ZnO/ITO, was 60-80 nm thick. The active layer annealed at different temperature (100-160 °C) for 20 minutes. Finally, on top of active layer, the MoO₃ (10 nm) followed by Ag (100 nm) film were deposited by thermal evaporator. The 4.5 mm² was the active area. The devices named as FBTSCN-IDT/BTSCN-IDT: PM6 CB and FBTSCN-IDT/BTSCN-IDT: PM6 CF throughout the manuscript for as-cast (chlorobenzene) and 140 °C (Chloroform) thermal annealing, respectively.

Characterization of solar cells devices:

The J-V characteristics of the OSCs devices under 1 Sun, were measured using Keithley 2400, and class AAA solar simulator (Newport Oriel Sol3A). The 1 Sun irradiation system is calibrated by using standard silicon solar cells. For indoor, the set-up built by using fluorescent lamp was used. The lux meter was used to measure the lamp intensity and the devices were measured under 1000 lux with an irradiance of 278.7 μW/cm². External quantum efficiency (EQE) was obtained using a QE X10 system (PV measurement), between 350 and 800 nm wavelength. The power density of the light was calibrated by using silicon photodiode.

Charge carrier mobility calculation data fitting

The applied SCLS question is given below

$$J_{SCLC} d = \frac{9}{8} \varepsilon_o \varepsilon_r \mu_o \exp(0.89\beta\sqrt{F}) F^2$$

Where J_{sclc} = SCLC current density, d = active layer thickness, ϵ_0 = vacuum permittivity, ϵ_r = relative permittivity of polymer, μ_0 = zero field mobility, β = field dependent coefficient, and F = electric field. Table S5 summarized the fitted value of β in the supporting information.

Synthesis

Sodium 2,2-dicyanoethene-1,1-bis(thiolate) (1)

To a solution of sodium hydroxide (3.30 g, 82.51 mmol) in ethanol (40 ml) at 0 °C was added malononitrile (2.68 g, 40.57 mmol) in one portion and the reaction stirred at 0 °C for 1 h. Carbon disulfide (2.50 ml, 41.57 mmol) was then added dropwise and the reaction mixture became white slurry. The reaction mixture was stirred at room temperature for 16 h, filtered and washed with ethanol, yielding white powder (4.16 g, yield: 54%). ^{13}C NMR (101 MHz, DMSO) δ 225.24, 124.04, 67.50 ppm. MS (m/z): $[\text{M}^+]$ calcd. for $\text{C}_4\text{N}_2\text{Na}_2\text{S}_2$ (M-Na): 140.9581, Found: 140.9588 (ESI). FTIR ($\nu \text{ cm}^{-1}$): 2171.2 $\{\nu(\text{CN})$ stretching $\}$, 1338.1 $\{\nu(\text{C}=\text{C})$ absorption band $\}$, 948.6 $\{\nu(=\text{CS}_2)$ group $\}$, 880.6 $\{\nu(\text{C}-\text{S})$ band $\}$.

4,4,9,9-Tetraoctyl-4,9-dihydro-s-indaceno[1,2-b:5,6-b']dithiophene (4)

To a solution of 4,9-dihydro-s-indaceno[1,2-b:5,6-b']dithiophene (0.51 g, 1.88 mmol) in anhydrous DMSO under nitrogen was added sodium tert-butoxide (1.09 g, 11.34 mmol) in portions. The reaction mixture was heated at 80 °C for one h before 1-bromooctane (2.19 g, 11.34 mmol) was injected dropwise, and stirred at 90 °C for 16 h. After cooling to room temperature, the crude product was quenched with water, extracted with chloroform, washed with brine and dried with magnesium sulfate. After removing the solvent under reduced pressure, the crude product was further purified using silica gel column chromatography with hexane as the eluent, yielding light yellow oil (0.73 g, yield: 54%). ^1H NMR (400 MHz, CDCl_3) δ 7.28 (s, 2H), 7.25 (d, $J = 4.95$ Hz, 2H), 6.96 (d, $J = 4.75$ Hz, 2H), 2.01-1.81 (m, 8H), 1.20-1.10 (m, 48H), 0.82 (t, $J = 6.99$ Hz, 12H) ppm. ^{13}C NMR (101 MHz, CDCl_3) δ 155.25, 153.39, 141.82, 135.74, 126.24, 121.85, 113.28, 77.48, 77.16, 76.84, 53.82, 39.31, 31.97, 30.18, 29.46, 29.37, 24.33, 22.75, 14.21 ppm.

(4,4,9,9-Tetraoctyl-4,9-dihydro-s-indaceno[1,2-b:5,6-b']dithiophene-2,7-diyl)bis(trimethylstannane) (5)

To a solution of compound 3 (163.20 mg, 0.23 mmol) in anhydrous THF (20 ml) at -78 °C under nitrogen was added n-butyllithium (2.5 M in hexanes, 0.1 ml, 0.25 mmol) dropwise. The reaction mixture was stirred at -78 °C for 1 h before trimethyltin chloride (1M in hexanes, 0.7

ml, 0.7 mmol) was injected dropwise, then warmed to room temperature and stirred for 16 h. After reaction, the mixture was quenched with water, extracted with dichloromethane, washed with brine and dried with magnesium sulfate. The solvent was removed under reduced pressure, yielding light yellow oil (176 mg, yield: 74%). ¹H NMR (400 MHz, CDCl₃) δ 7.32 (s, 2H), 7.04 (s, 2H), 2.06-1.87 (m, 8H), 1.22-1.16 (m, 48H), 0.87 (t, *J* = 6.98 Hz, 12H), 0.45 (m, 18H) ppm.

2-(4-Bromo-[1,3]dithiolo[4',5':3,4]benzo[1,2-c][1,2,5]thiadiazol-7-ylidene)malononitrile (BTSCN)

A solution of compound 5a (708 mg, 2.27 mmol) and compound 1 (633.8 mg, 3.40 mmol) in anhydrous DMSO (15 ml) was heated at 60 °C under nitrogen for 16 h. After cooling to room temperature, the reaction mixture was added to 100 ml water, extracted with ethyl acetate, washed with brine and dried with magnesium sulfate. After removing the solvent under reduced pressure, the crude product was further purified using silica gel column chromatography with the mixture of petroleum ether and dichloromethane (1:2, v/v) as the eluent, yielding light yellow powder (361.56 mg, yield: 45%). ¹H NMR (400 MHz, CDCl₃) δ 7.99 (s, 1H) ppm. ¹³C NMR (101 MHz, CDCl₃) δ 177.81, 152.58, 147.74, 136.56, 125.02, 115.40, 112.28, 67.34. MS (*m/z*): [*M*⁺] calcd. for C₁₀HBrN₄S₃: 353.23, Found: 353.8526 (ESI). FTIR (ν cm⁻¹): 2221.5 {ν(CN) stretching}, 1476.0 {ν(C=C) absorption band}, 872.2 {ν(C-S) band}.

2-(4-Bromo-5-fluoro-[1,3]dithiolo[4',5':3,4]benzo[1,2-c][1,2,5]thiadiazol-7-ylidene)malononitrile (FBTSCN)

FBTSCN was synthesized according to the same procedures as BTSCN (yield: 55%). ¹³C NMR (101 MHz, CDCl₃) δ 176.85, 154.42 (d, ¹*J*_{C-F} = 255.23 Hz), 153.38 (d, ³*J*_{C-F} = 5.17 Hz), 144.79, 128.10 (d, ²*J*_{C-F} = 26.22 Hz), 126.18 (d, ³*J*_{C-F} = 4.38 Hz), 111.98, 111.95, 99.37 (d, ²*J*_{C-F} = 22.75 Hz), 68.92 ppm. ¹⁹F NMR (377 MHz, Toluene) δ -102.64 ppm. MS (*m/z*): [*M*⁺] calcd. for C₁₀BrFN₄S₃: 371.22, Found: 371.8434 (ESI). FTIR (ν cm⁻¹): 2214.0 {ν(CN) stretching}, 1461.1 {ν(C=C) absorption band}, 875.2 {ν(C-S) band}.

2,2'-((4,4,9,9-Tetraoctyl-4,9-dihydro-*s*-indaceno[1,2-*b*:5,6-*b'*]dithiophene-2,7-diyl)bis([1,3]dithiolo[4',5':3,4]benzo[1,2-*c*][1,2,5]thiadiazole-4-yl-7-ylidene))dimalononitrile (BTSCN-IDT)

A solution of compound BTSCN (167 mg, 0.47 mmol), compound 4 (224 mg, 0.22 mmol) and P(PPh₃)₄ (24.9 mg, 0.02 mmol) in the mixture of anhydrous toluene (10 ml) and DMF (2 ml

under nitrogen was heated at 100 °C for 48 h. After cooling to room temperature, the crude product was quenched with water, extracted with dichloromethane, washed with brine and dried with magnesium sulfate. After removing the solvent, the crude product was further purified using silica gel column chromatography with the mixture of petroleum ether and dichloromethane (1:1, v/v) as the eluent, yielding red solid (176.24 mg, yield: 65%). ¹H NMR (400 MHz, CDCl₃) δ 8.11 (s, 2H), 7.96 (s, 2H), 7.42 (s, 2H), 2.15-1.93 (m, 8H), 1.25-1.11 (m, 48H), 0.76 (t, *J* = 6.75 Hz, 12H). ¹³C NMR (101 MHz, CDCl₃) δ 179.01, 156.93, 154.22, 151.26, 149.14, 145.99, 138.97, 137.45, 136.33, 129.24, 124.19, 122.53, 116.42, 114.12, 112.94, 112.71, 66.17, 54.60, 39.25, 31.93, 30.11, 29.45, 24.42, 22.74, 14.21. MS (*m/z*): [M⁺] calcd. for C₆₈H₇₄N₈S₈: 1259.88, Found: 1259.0 (MALDI-TOF).

2,2'-((4,4,9,9-Tetraoctyl-4,9-dihydro-s-indaceno[1,2-b:5,6-b']dithiophene-2,7-diyl)bis(5-fluoro-[1,3]dithiolo[4',5':3,4]benzo[1,2-c][1,2,5]thiadiazole-4-yl-7-ylidene))dimalononitrile (FBTSCN-IDT)

FBTSCN-IDT was synthesized using similar procedures as BTSCN-IDT (yield: 67%). ¹H NMR (400 MHz, CDCl₃) δ 8.22 (s, 2H), 7.47 (s, 2H), 2.16-1.93 (m, 8H), 1.21-1.12 (m, 48H), 0.79 (t, *J* = 6.87 Hz, 12H). ¹³C NMR (101 MHz, CDCl₃) δ 178.00, 156.30, 154.50, 152.80, 152.48, 152.39, 150.25, 147.58 , , 147.50, 145.79, 136.47, 132.37, 132.30 , 129.38, 126.57, 126.47 , 122.14, 122.09, 114.57, 114.44 114.33, 112.46, 112.35 , 67.65, 54.57, 39.27, 31.93, 30.09, 29.32, 24.44, 22.73, 14.18. ¹⁹F NMR (377 MHz, CDCl₃) δ -107.53. MS (*m/z*): [M⁺] calcd. for C₆₈H₇₂F₂N₈S₈: 1295.86, Found: 1295.1 (MALDI-TOF).

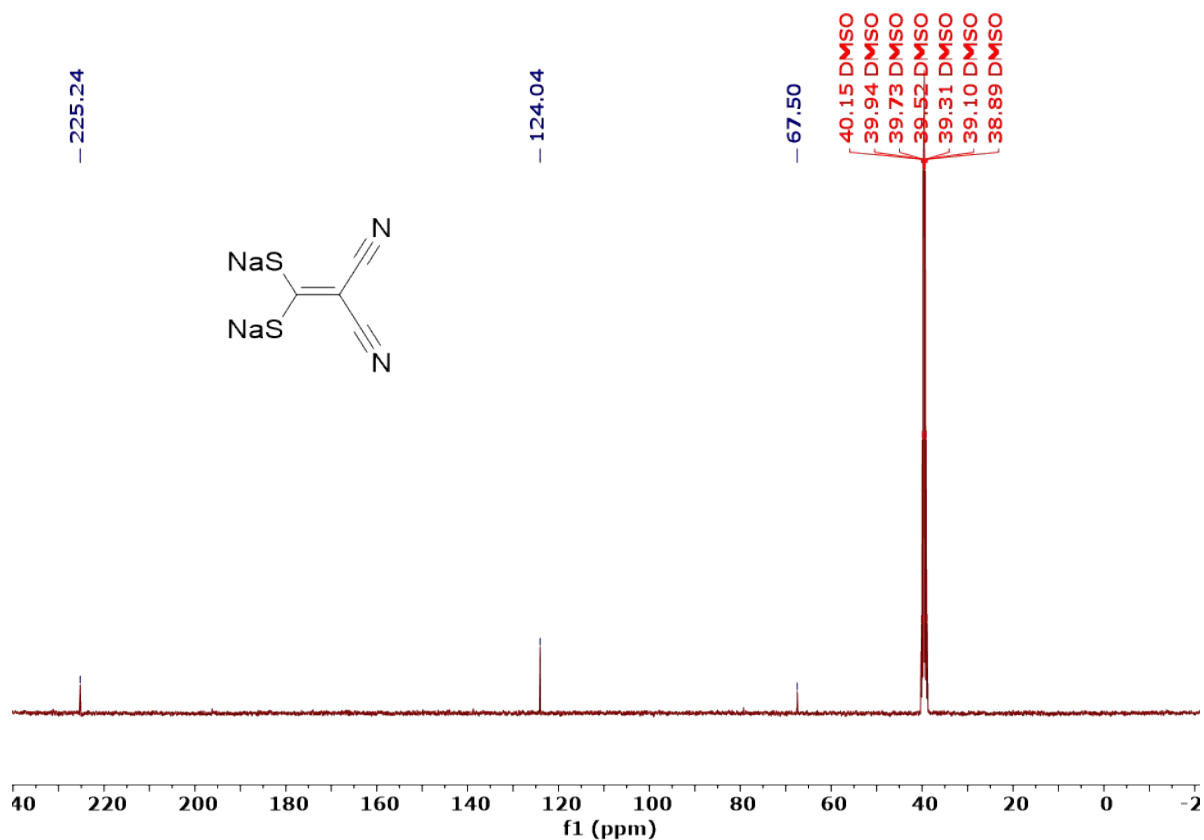


Figure S1. ^{13}C NMR spectrum of compound 1.

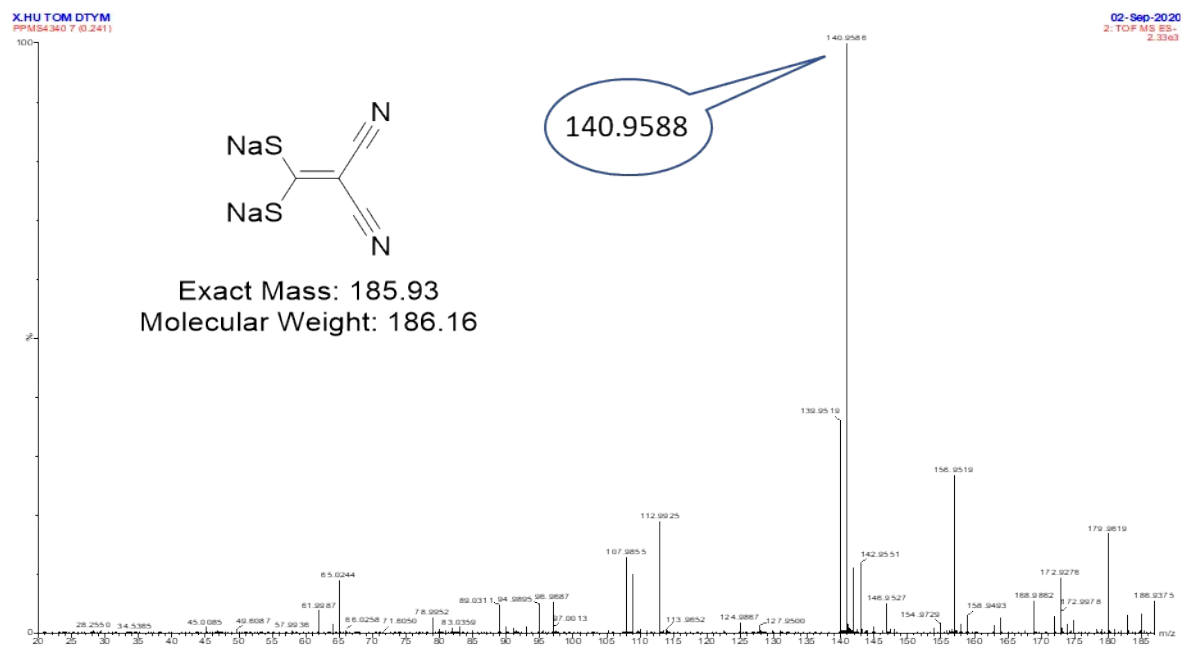


Figure S2. Mass spectrum of compound 1.

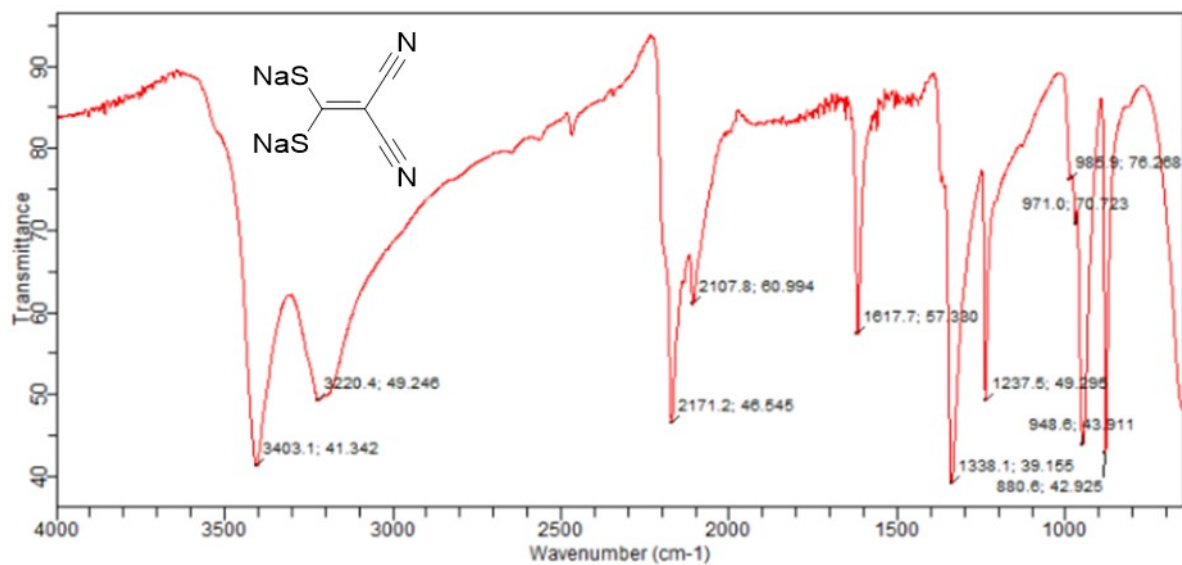


Figure S3. FTIR spectrum of compound 1.

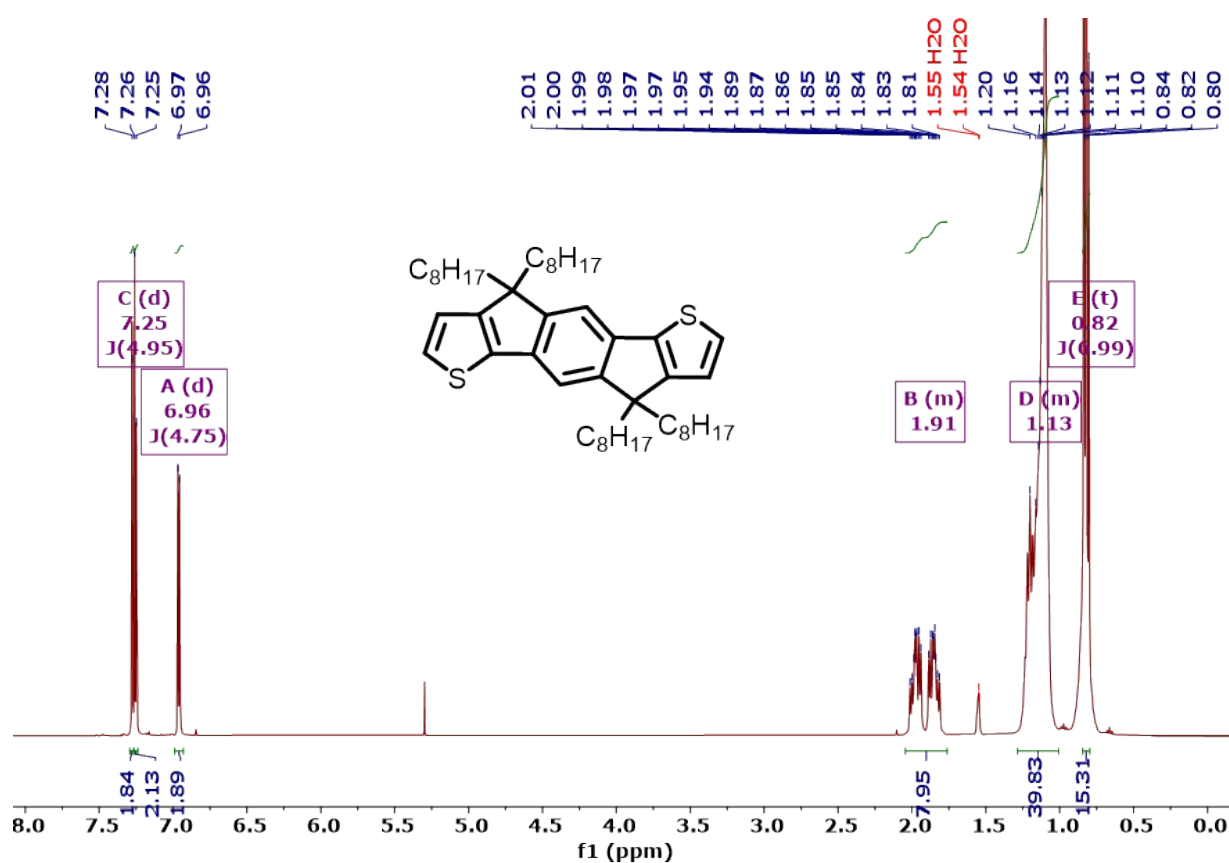


Figure S4. ¹H NMR spectrum of compound 4.

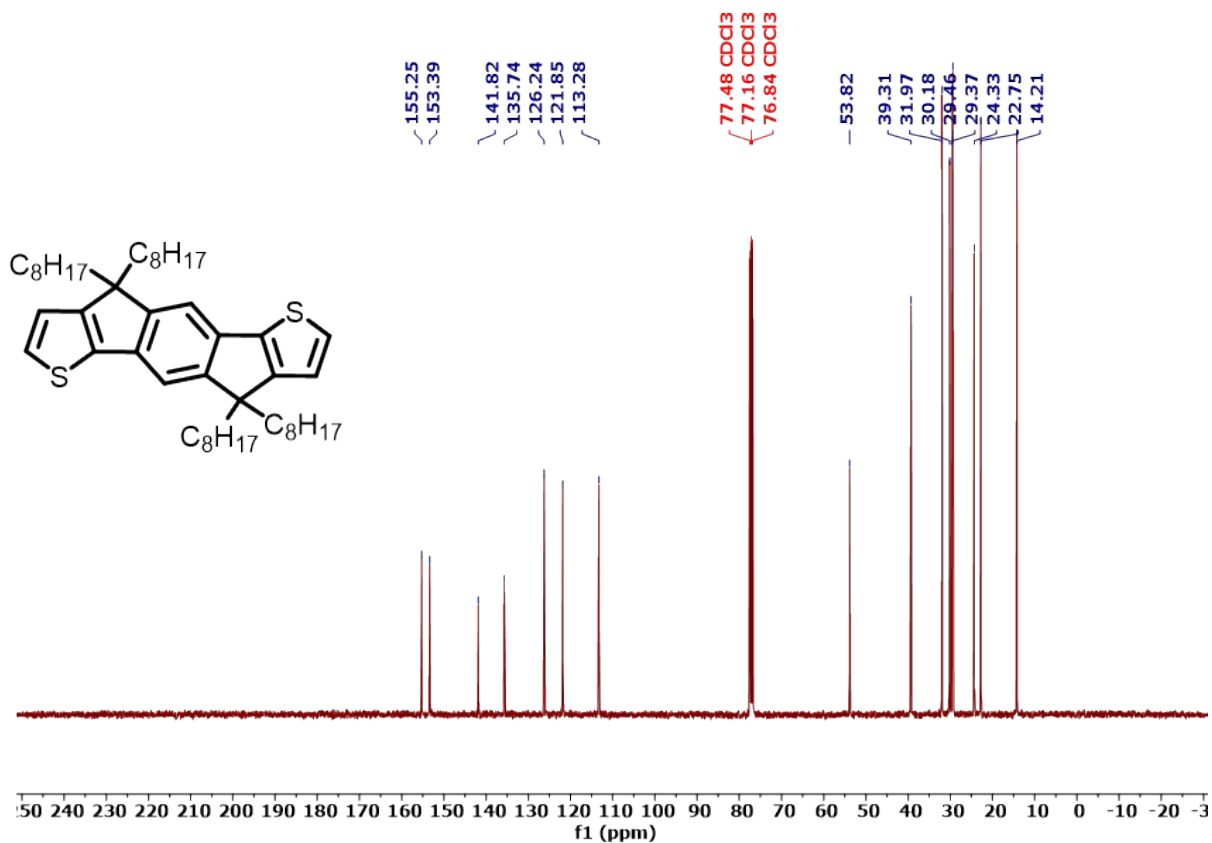


Figure S5. ¹³C NMR spectrum of compound 4.

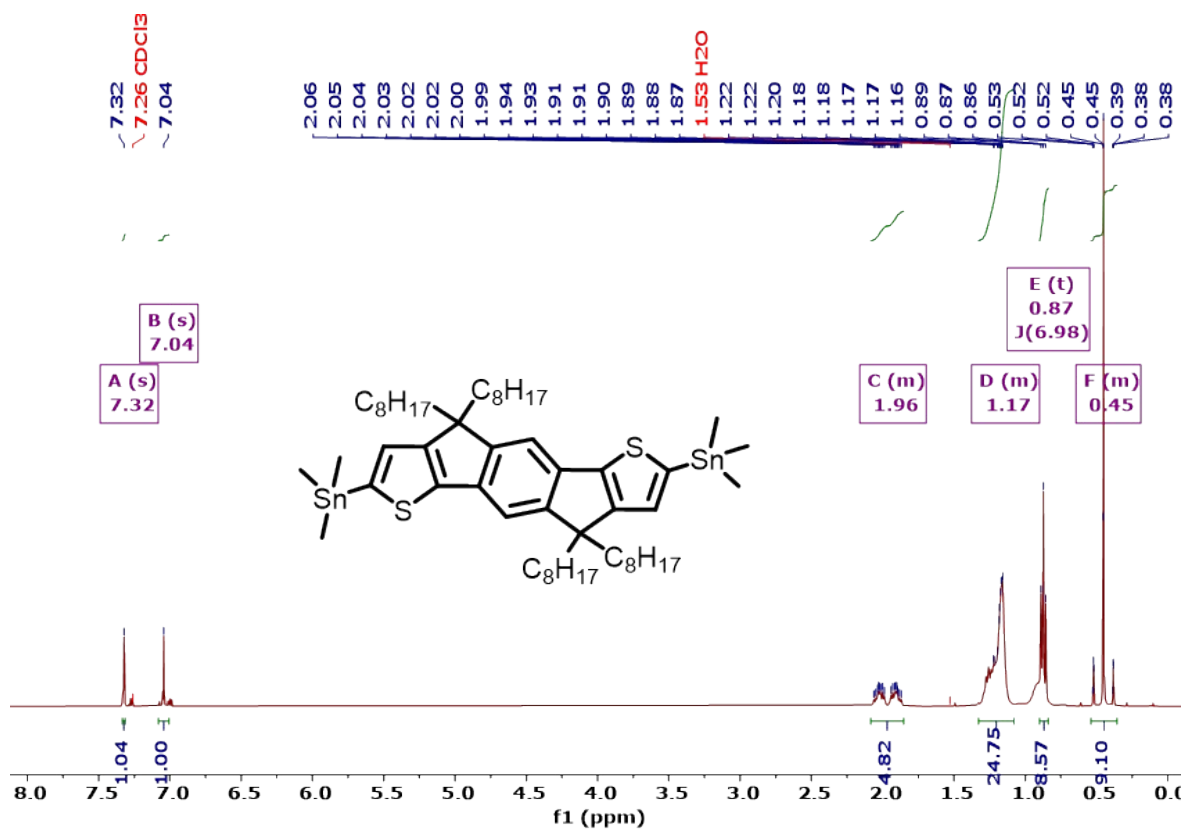


Figure S6. ¹H NMR spectrum of compound 5.

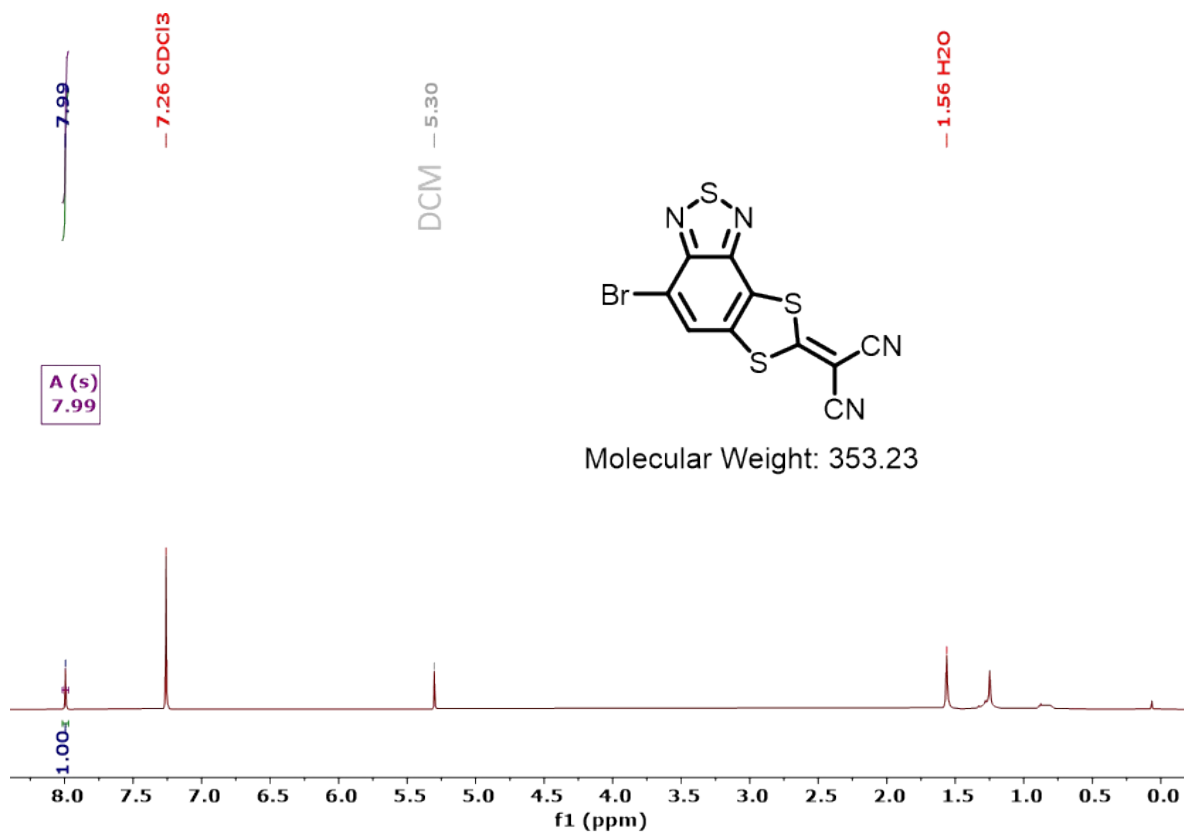


Figure S7. $^1\text{H NMR}$ spectrum of BTSCN.

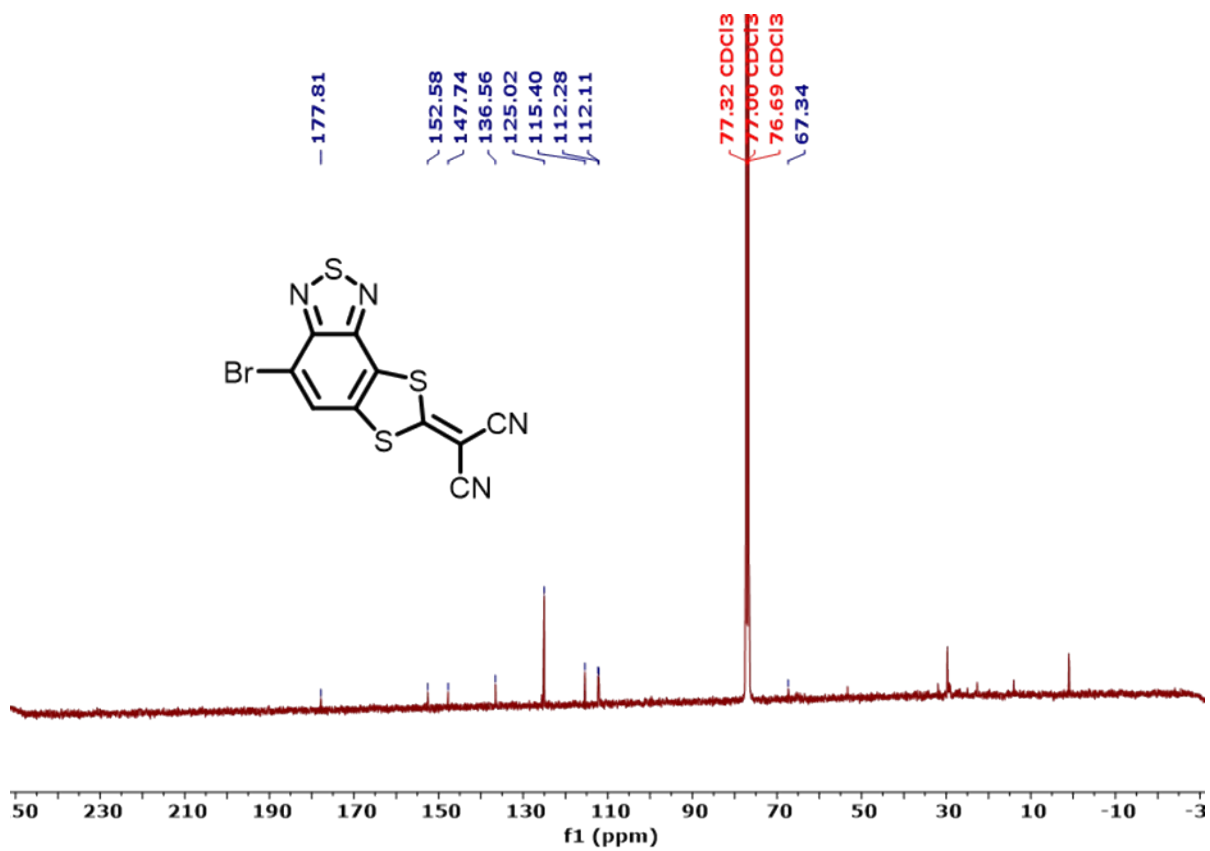


Figure S8. $^{13}\text{C NMR}$ spectrum of BTSCN.

121120_PPMSS484 #324 RT: 0.41 AV: 1 NL: 6.44E6
T: FTMS - p APCI corona Full ms [100.0000-800.0000]

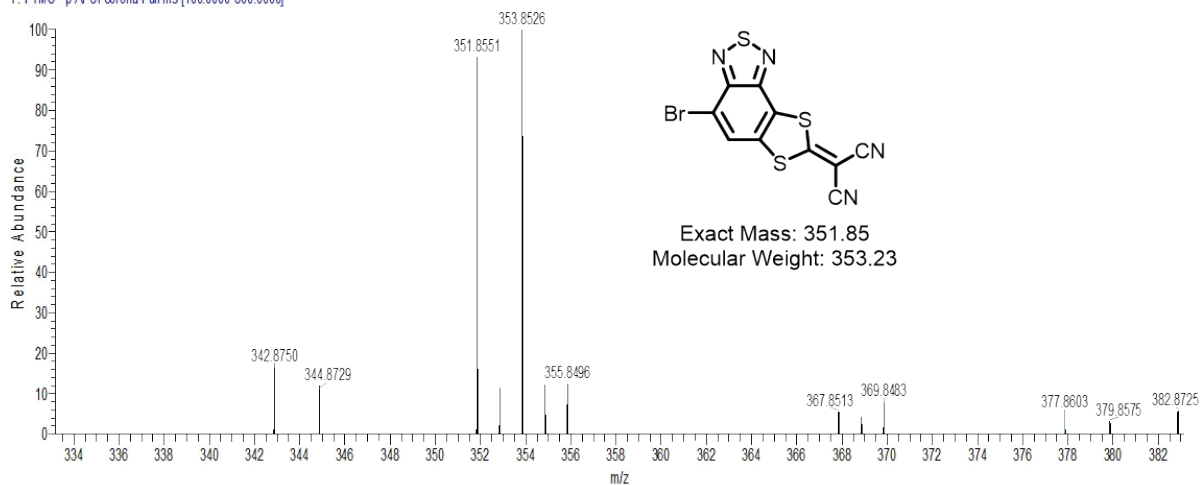


Figure S9. Mass spectrum of BTSCN.

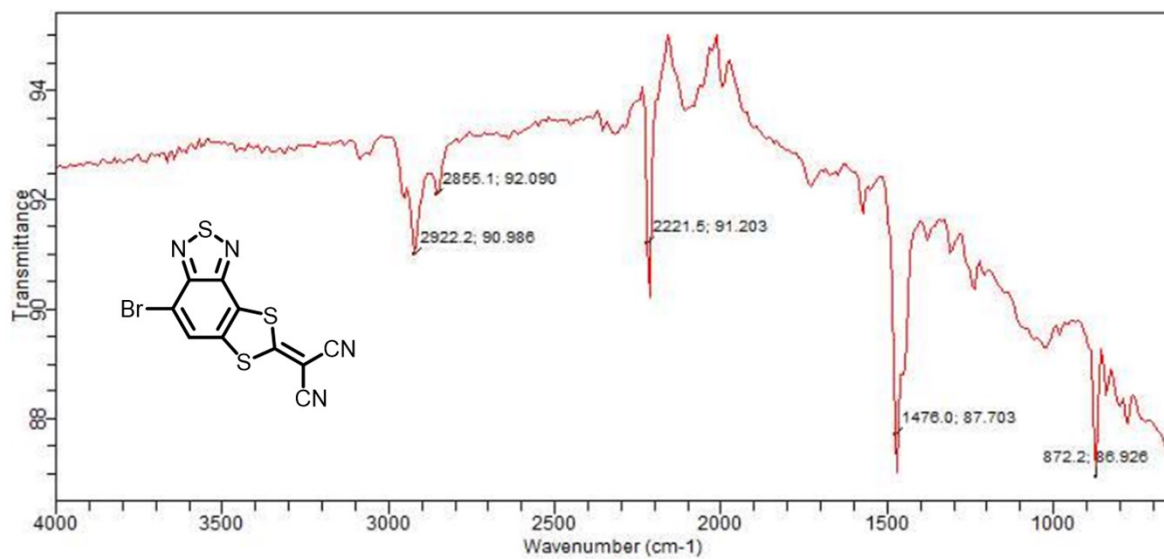


Figure S10. FTIR spectrum of BTSCN.

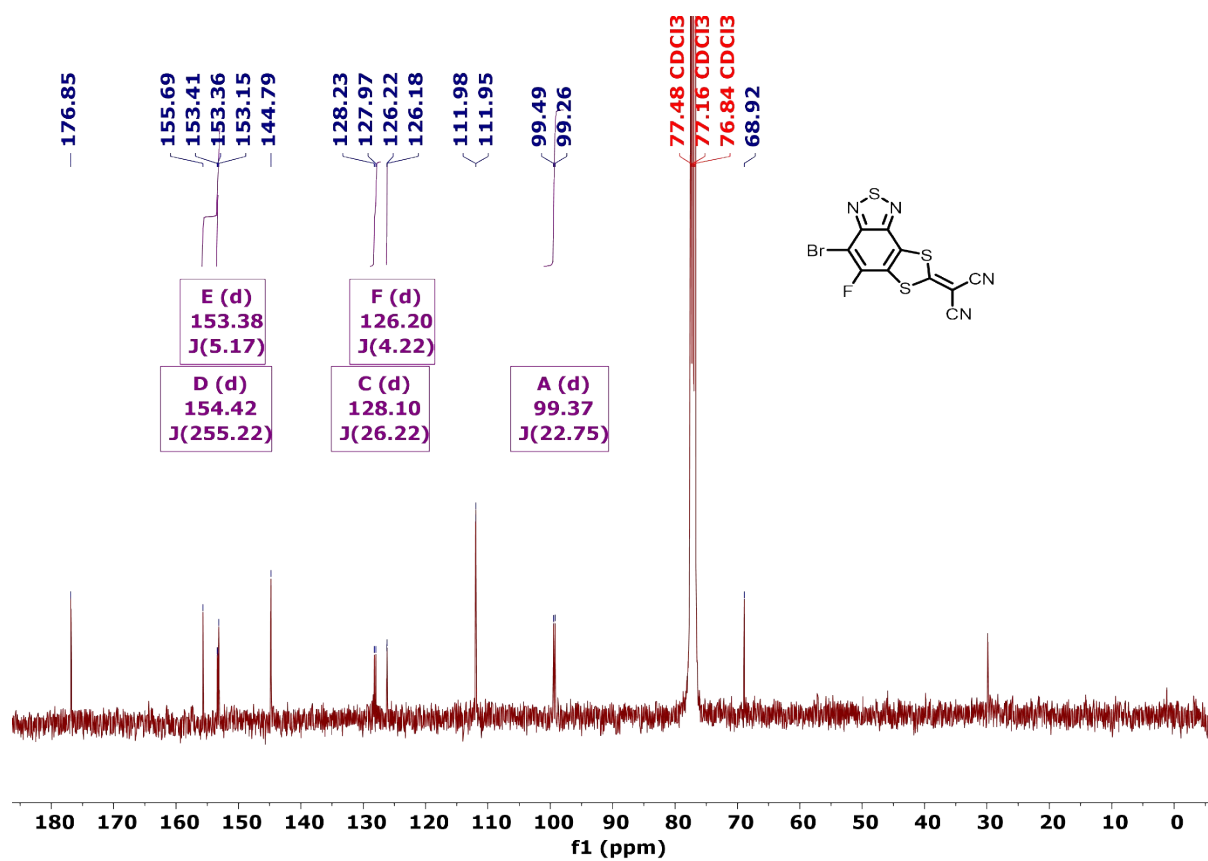


Figure S11. ¹³C NMR spectrum of FBTSCN.

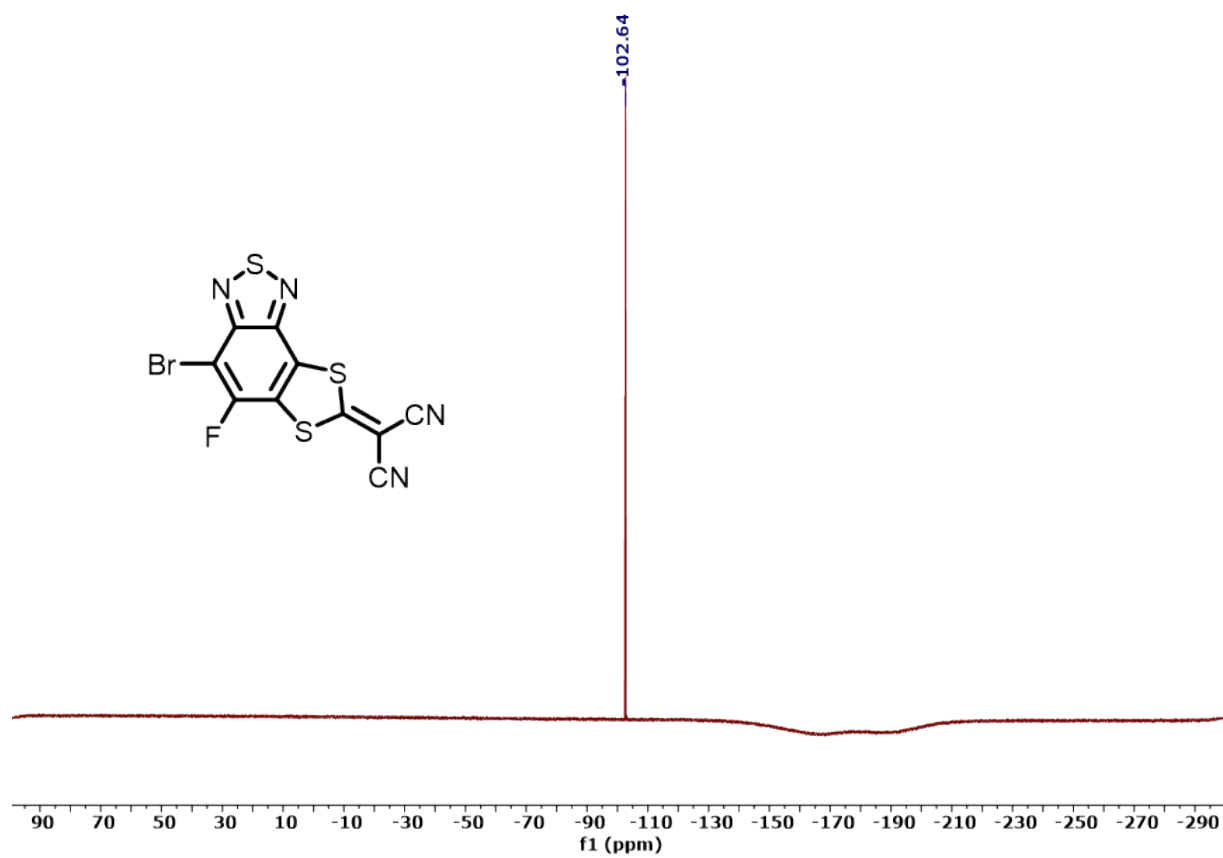


Figure S12. ¹⁹F NMR spectrum of FBTSCN.

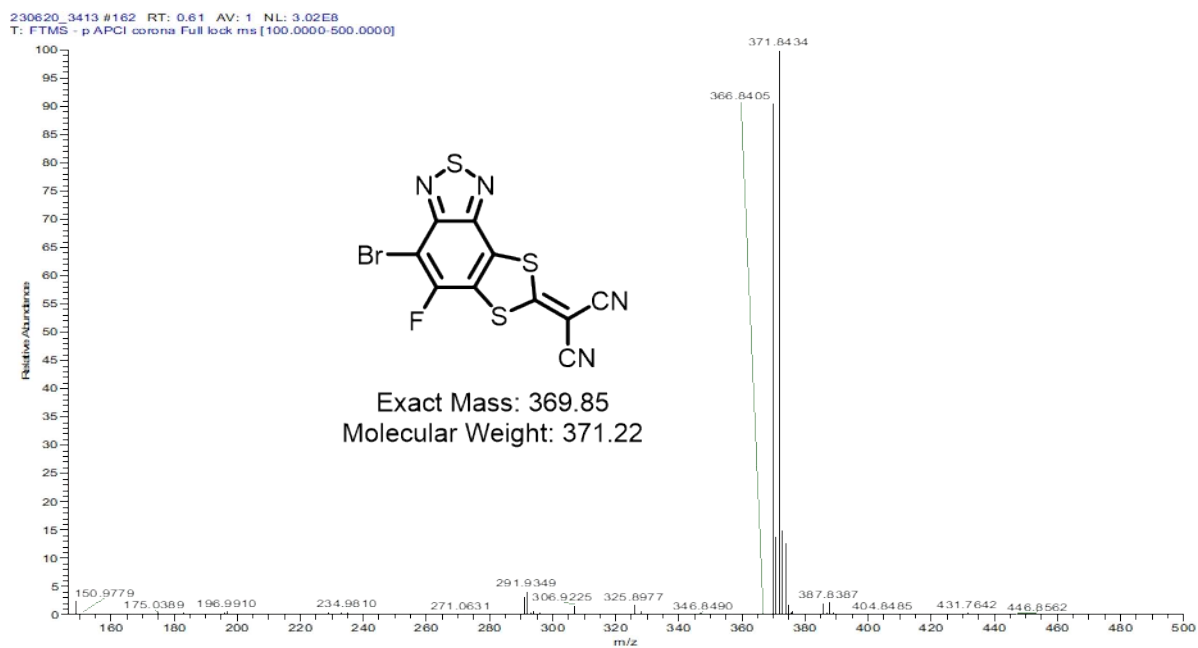


Figure S13. Mass spectrum of FBTSCN.

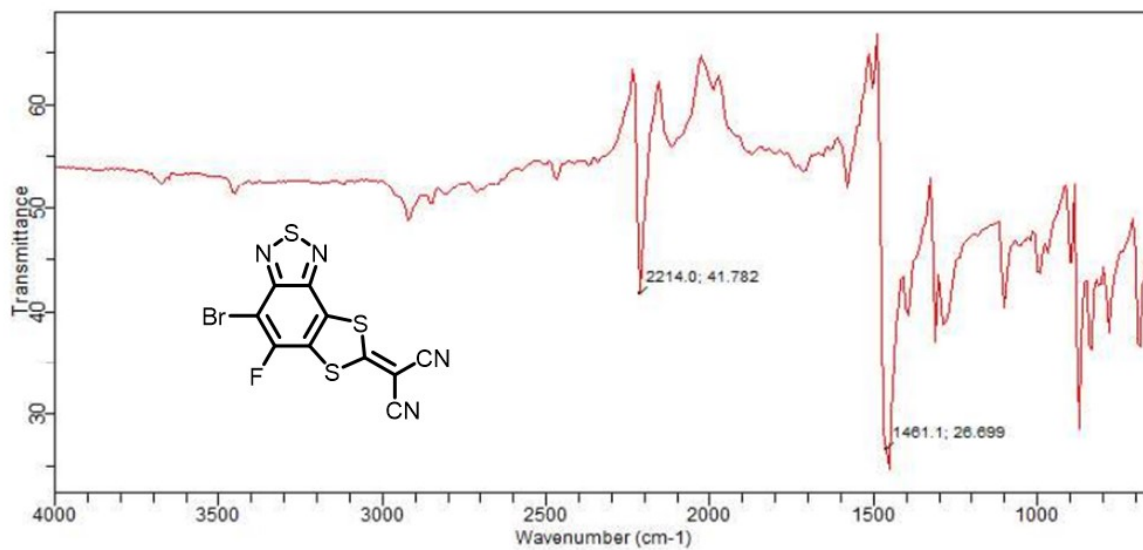


Figure S14. FTIR spectrum of FBTSCN.

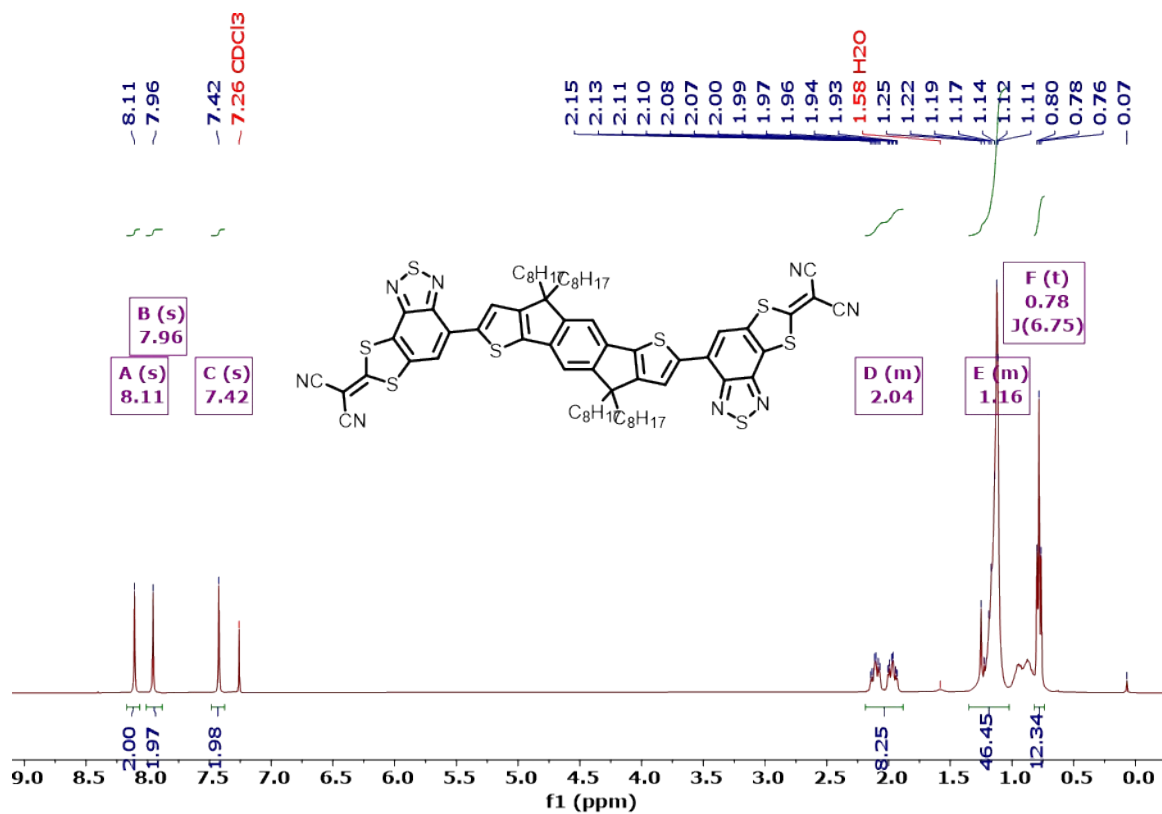


Figure S15. ¹H NMR spectrum of BTSCN-IDT.

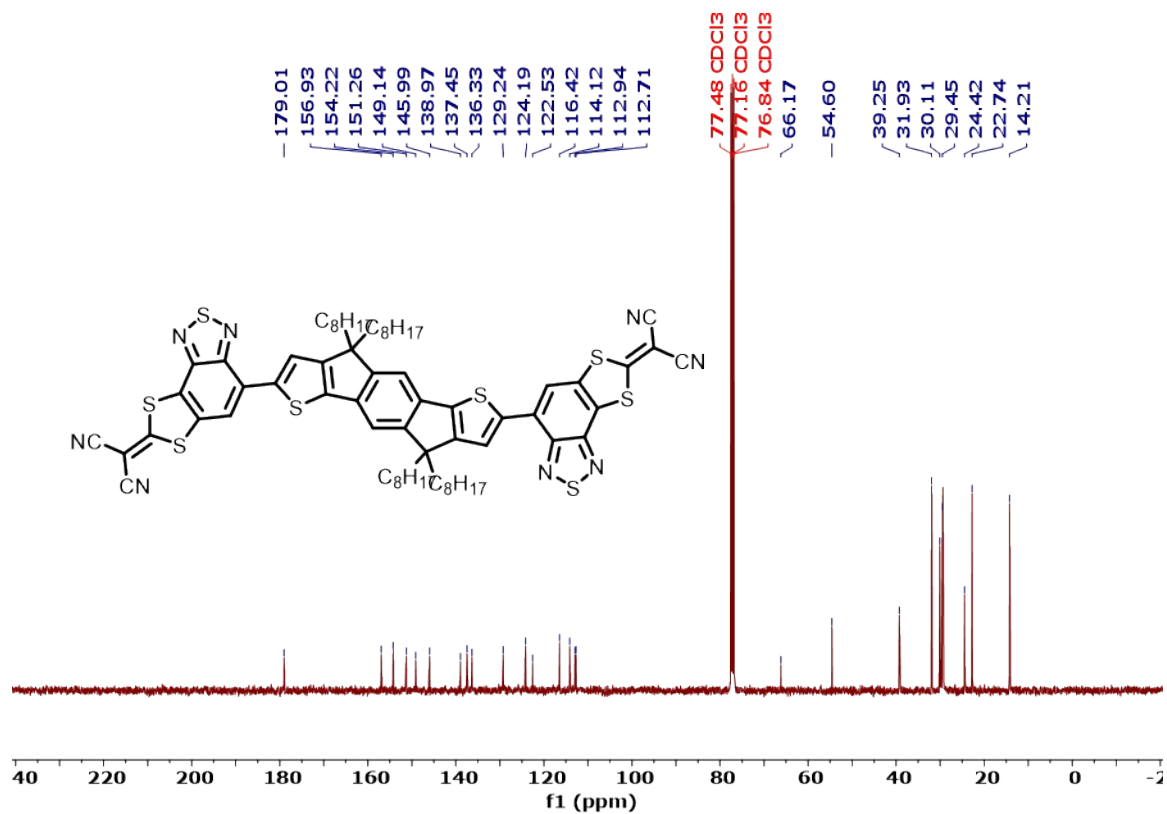


Figure S16. ¹³C NMR spectrum of BTSCN-IDT.

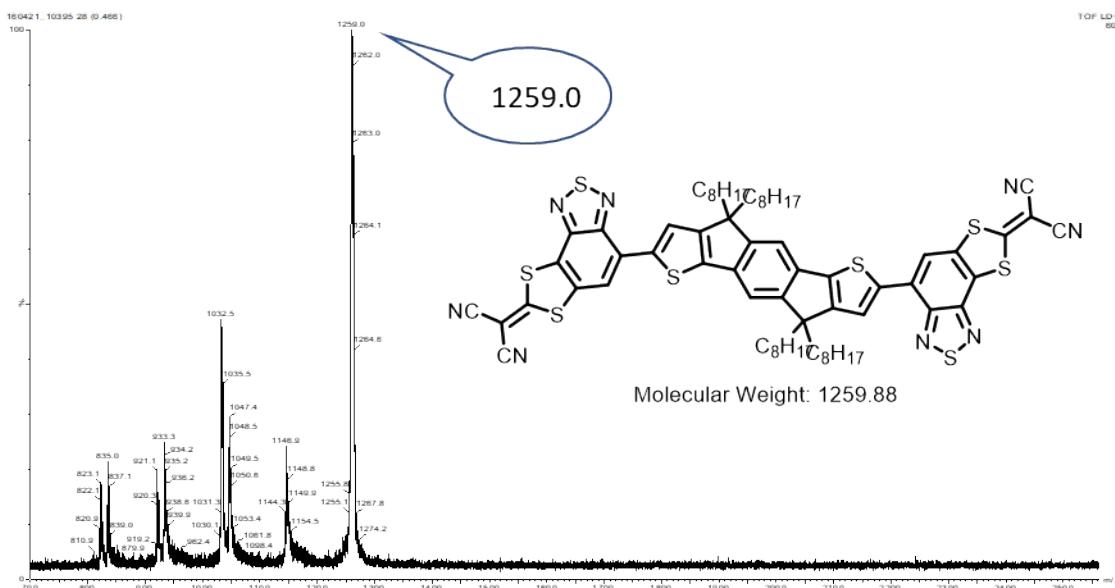


Figure S17. Mass spectrum of BTSCN-IDT.

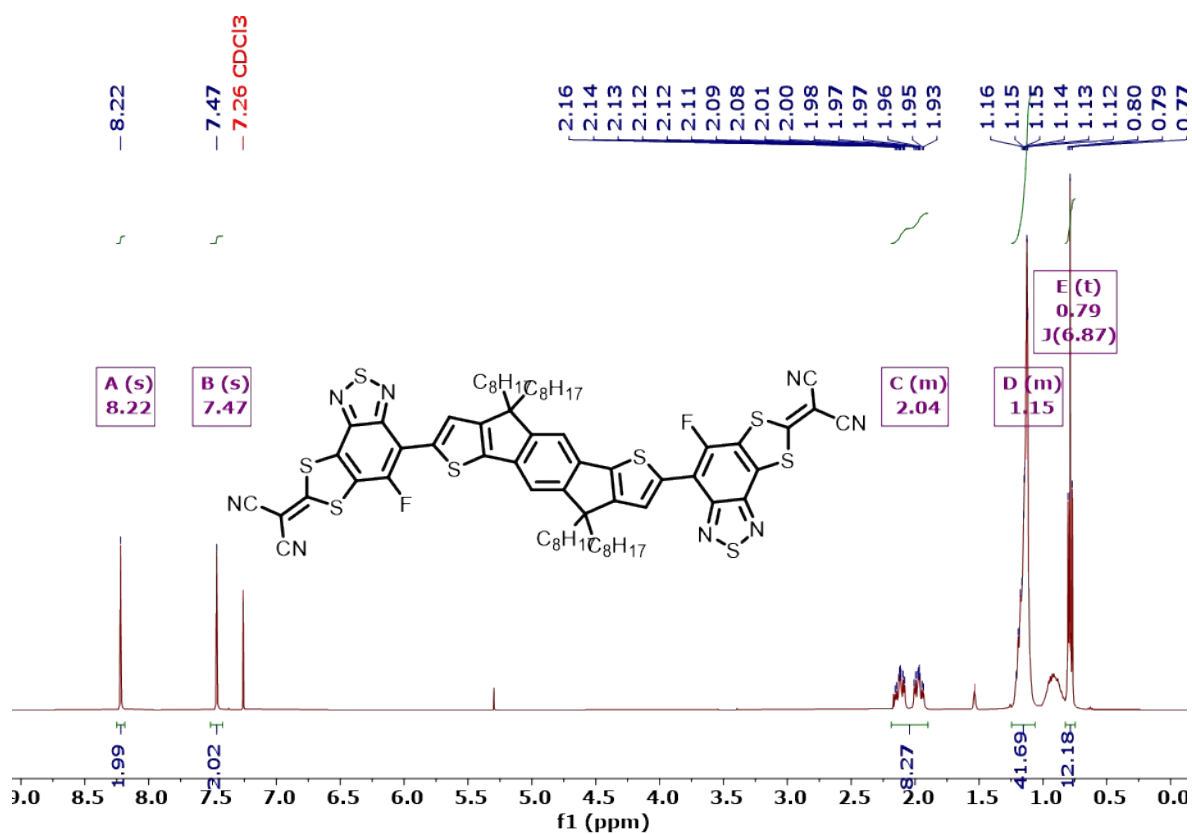


Figure S18. ¹H NMR spectrum of FBTSCN-IDT.

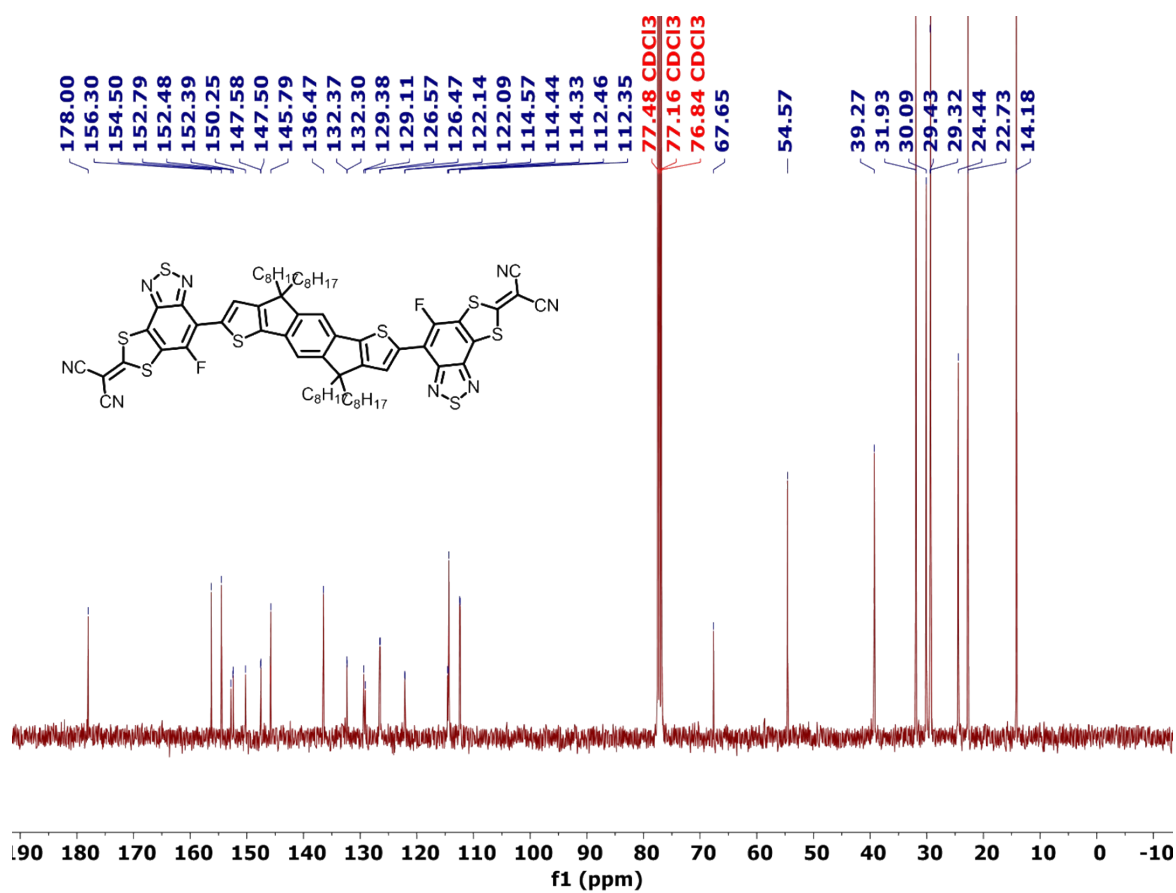


Figure S19. ¹³C NMR spectrum of FBTSCN-IDT.

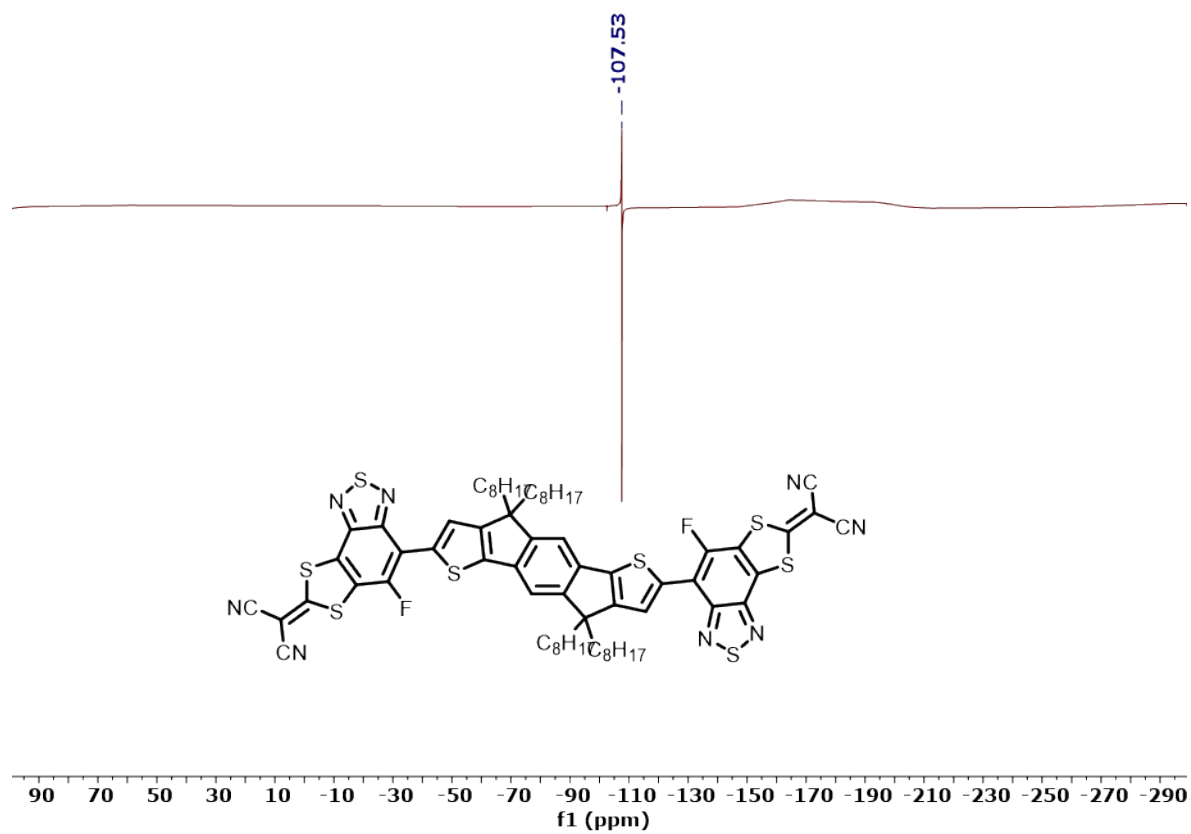


Figure S20. ¹⁹F NMR spectrum of FBTSCN-IDT.

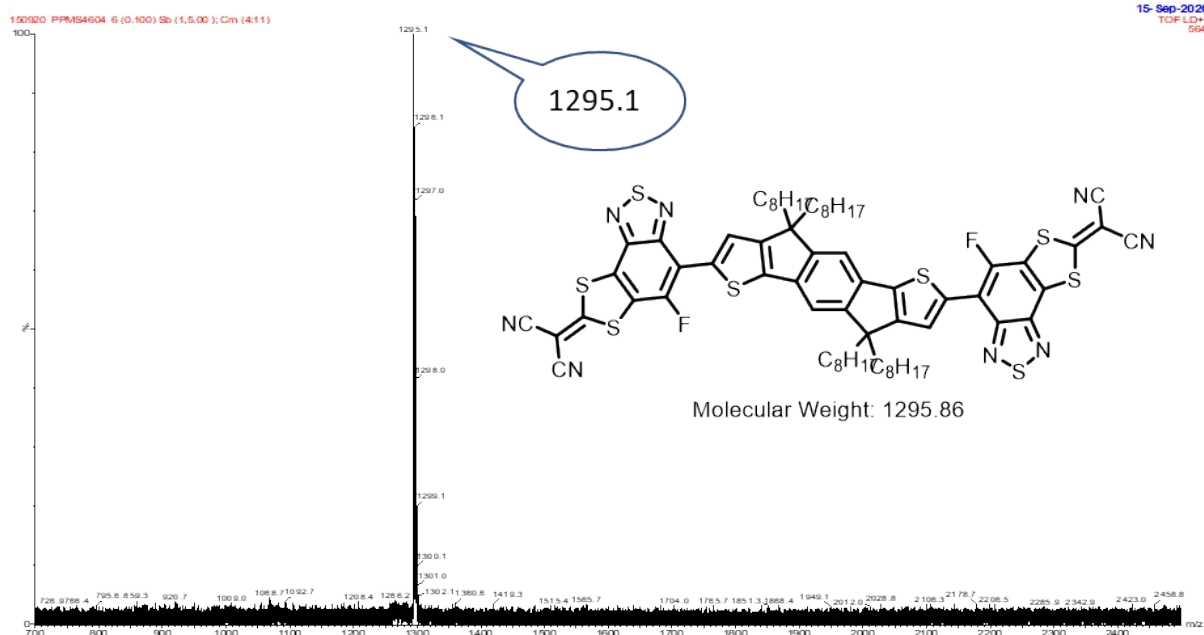


Figure S21. Mass spectrum of FBTSCN-IDT.

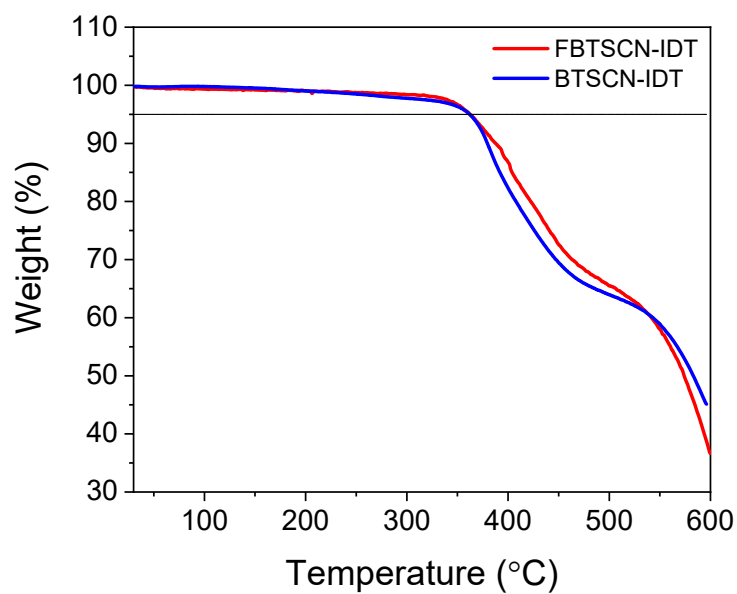


Figure S22. TGA traces of FBTSCN-IDT, BTSCN-IDT, heating rate 10 K/min.

The X-ray crystal structure of **3a**

Crystal data for 3a: C₁₀HBrN₄S₃, *M* = 353.24, monoclinic, *P*2₁/*c* (no. 14), *a* = 9.9571(4), *b* = 7.1731(2), *c* = 16.5511(6) Å, β = 104.644(4)°, *V* = 1143.74(8) Å³, *Z* = 4, *D*_c = 2.051 g cm⁻³, μ(Mo-Kα) = 4.123 mm⁻¹, *T* = 173 K, yellow platy needles, Agilent Xcalibur 3 E diffractometer; 2529 independent measured reflections (*R*_{int} = 0.0520), *F*² refinement,^[X1,X2] *R*₁(obs) = 0.0370, *wR*₂(all) = 0.0883, 2066 independent observed absorption-corrected reflections [*|F_o |* > 4σ(*|F_o |*)], completeness to θ_{full}(25.2°) = 100%, 163 parameters. CCDC 2164513.

The X-ray crystal structure of **3b**

Crystal data for 3b: C₁₀BrFN₄S₃, *M* = 371.23, orthorhombic, *Pbca* (no. 61), *a* = 13.3202(6), *b* = 15.6848(5), *c* = 22.7909(8) Å, *V* = 4761.6(3) Å³, *Z* = 16 [two independent molecules], *D*_c = 2.071 g cm⁻³, μ(Mo-Kα) = 3.979 mm⁻¹, *T* = 173 K, yellow blocks, Agilent Xcalibur 3 E diffractometer; 4815 independent measured reflections (*R*_{int} = 0.0208), *F*² refinement,^[X1,X2] *R*₁(obs) = 0.0382, *wR*₂(all) = 0.0926, 3200 independent observed absorption-corrected reflections [*|F_o |* > 4σ(*|F_o |*)], completeness to θ_{full}(25.2°) = 99.1%, 343 parameters. CCDC 2164514.

The structure of **3b** was found to contain two crystallographically independent molecules (**3b-A** and **3b-B**) in the asymmetric unit.

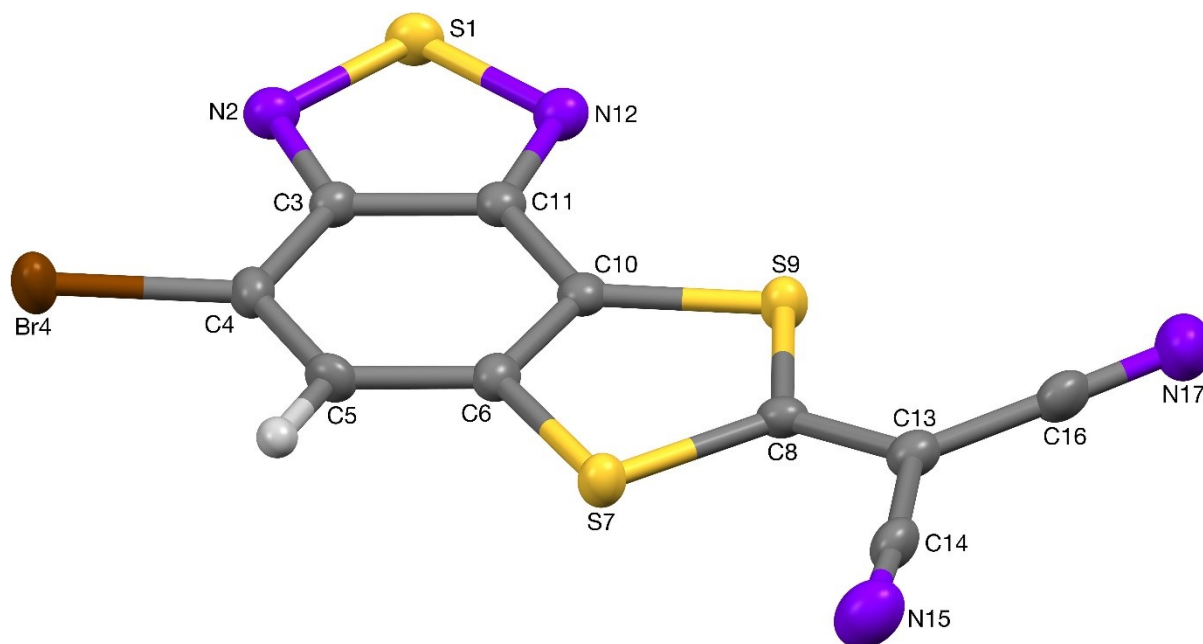


Figure S23. The crystal structure of **3a** (50% probability ellipsoids).

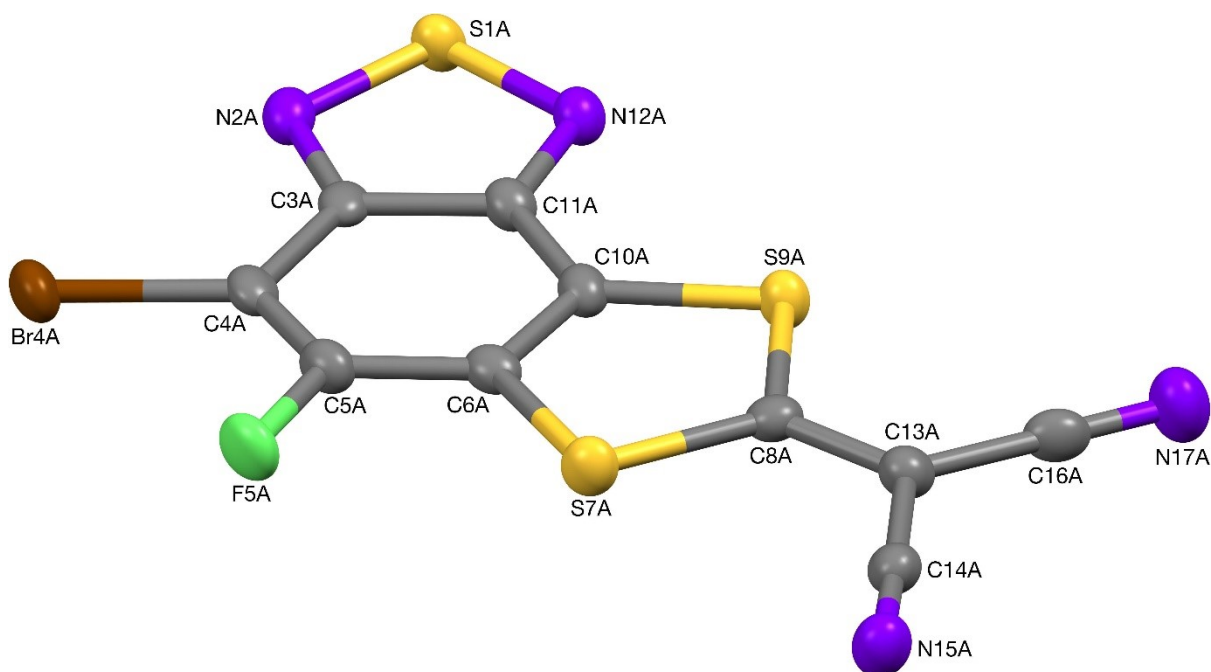


Figure S24. The structure of **3b-A**, one of the two independent molecules present in the crystal of **3b** (50% probability ellipsoids).

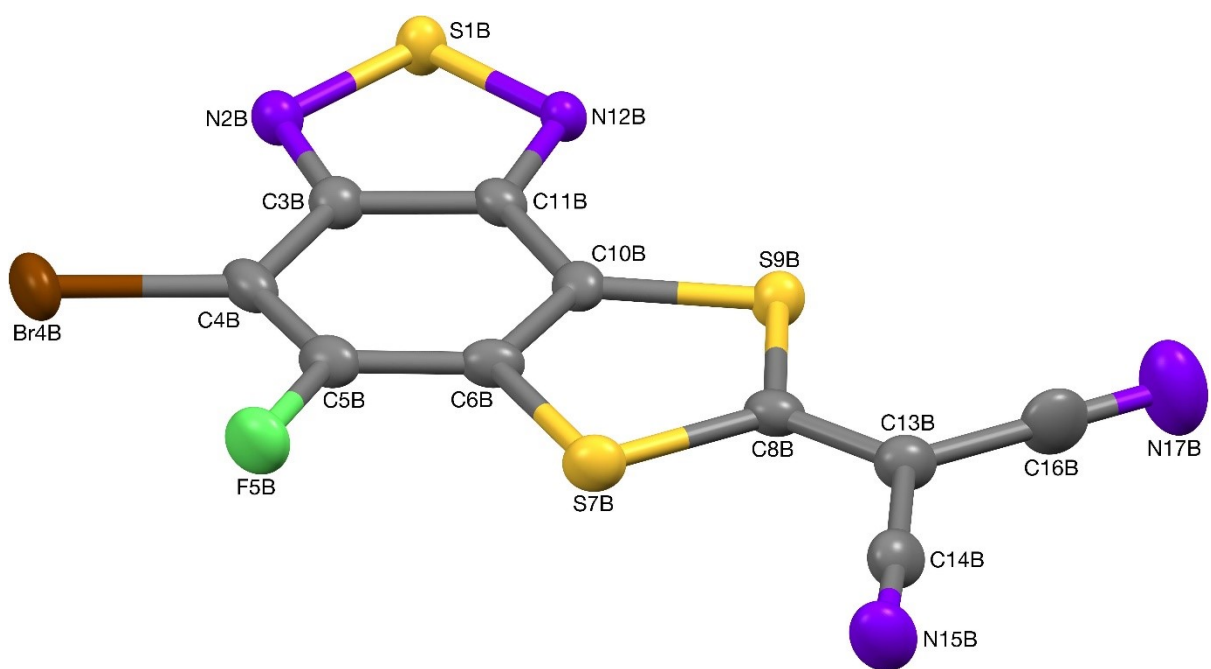


Figure S25. The structure of **3b-B**, one of the two independent molecules present in the crystal of **3b** (50% probability ellipsoids).

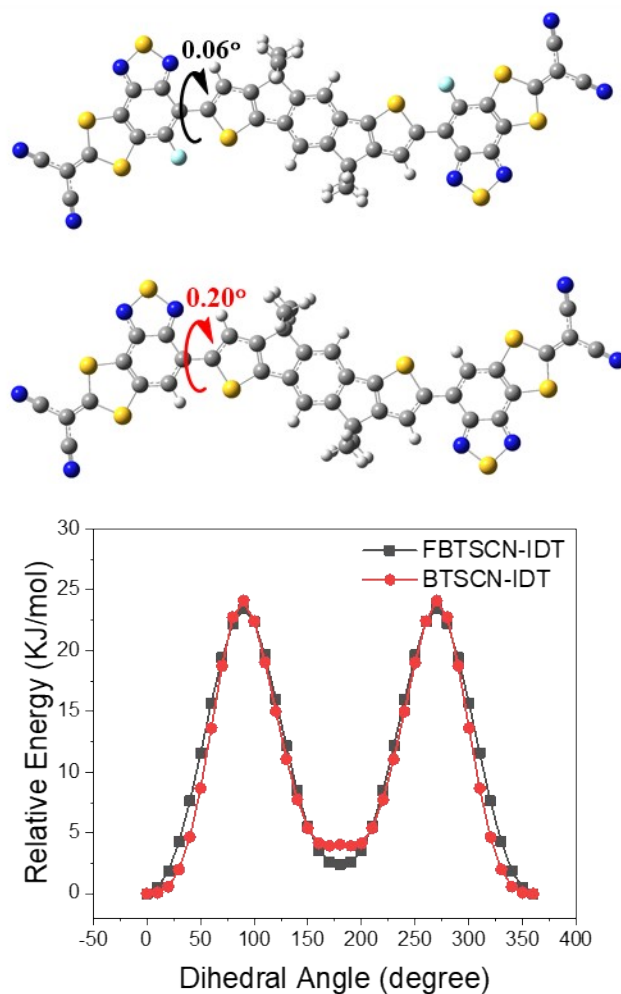


Figure S26. Optimized molecular structure and potential energy scan spectra of FBTSCN-IDT and BTSCN-IDT.

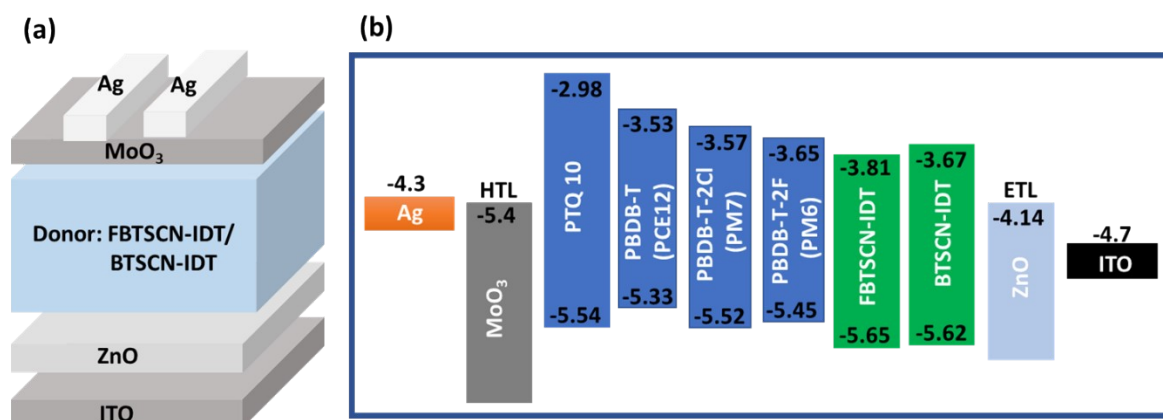


Figure S27. Fabricated device (a) structure and its (b) molecules energy level diagram (values in eV).

Table S1. OSCs device performance of PTQ-10/PBDB-T/PM6/PM7: FBTSCN-IDT photoactive layer-based device measurement under AM 1.5G.

Donors	Thermal annealing (°C)	V_{oc} (V)	J_{sc} (mA/cm ²)	FF (%)	PCE (%)
PTQ-10	As-cast	1.18±0.0148(1.20)	4.7±0.204(4.95)	36.16±1.075(37.23)	2.04±0.157(2.2)
	100	1.13±0.045(1.18)	6.2±0.380(6.58)	40.07±2.920(42.99)	2.91±0.386(3.3)
	120	1.074±0.006 (1.08)	7.4±0.620(8.08)	48.85±2.047(50.90)	4.05±0.450(4.5)
	140	1.04±0.0198(1.06)	3.9±1.597(5.49)	47.27±4.211(51.49)	2.12±0.873(3.00)
	160	1.00±0.0521(1.06)	5.5±0.264(5.80)	46.26±3.33(49.59)	2.50±0.199(2.7)
PBDB-T	As-cast	0.99±0.011(1.01)	3.9±0.171(4.08)	37.13±1.389(38.51)	1.49±0.067(1.56)
	100	1.00±0.008(1.01)	6.8±0.450(7.30)	37.94±0.940(38.88)	5.65±0.146(2.8)
	120	0.97±0.004 (0.97)	10.1±0.664(10.78)	45.36±1.118(46.47)	4.37±0.256(4.63)
	140	0.91±0.005(0.92)	11.1±0.524(11.63)	49.54±1.04(50.58)	4.86±0.336(5.2)
	160	0.90±0.004(0.91)	12.1±0.846(13.01)	46.76±0.901(47.67)	5.21±0.347(5.56)
PM6	As-cast	1.20±0.005(1.11)	5.5±0.517(6.11)	36.12±0.539(36.66)	2.27±0.221(2.5)
	100	1.08±0.011(1.10)	7.0±0.015(7.11)	38.10±0.622(38.73)	2.94±0.074(3.0)
	120	1.04±0.003(1.05)	10.3±0.601(10.95)	46.01±1.276(47.28)	4.90±0.274(5.2)
	140	1.00±0.002(1.01)	10.7±0.618(11.40)	51.24±0.795(52.03)	5.57±0.329(5.90)
	160	1.00±0.002(1.01)	9.9±0.112(10.09)	49.53±1.061(50.59)	4.94±0.170(5.11)
PM7	As-cast	1.14±0.021(1.18)	4.8±0.32(5.20)	37.58±1.66(39.24)	2.13±0.162(2.3)
	100	1.12±0.011(1.14)	6.4±0.369(6.80)	40.01±2.33(42.34)	2.97±0.300(3.27)
	120	1.05±0.013(1.07)	7.0±0.194(7.20)	47.48±2.15(49.63)	3.57±0.232(3.8)
	140	1.04±0.018(1.06)	6.9±0.12(7.03)	52.61±3.46(56.07)	3.80±0.301(4.1)
	160	1.03±0.018(1.05)	8.3±1.18(9.51)	50.86±2.97(53.83)	4.25±0.353(4.6)

Table S2. Summary of photovoltaic performance of FBTSCN-IDT/BTSCN-IDT: PM6 photoactive layer-based device measurement under 1 Sun.

Active Layer	Thermal annealing (°C)	V_{oc} (V)	J_{sc} (mA/cm ²)	FF (%)	PCE (%)
PM6: FBTSCN-IDT, Chlorobenzene	As-cast	1.04±0.024(1.07)	9.3±0.340(9.70)	57.66±3.922(61.5)	5.69±0.61 (6.3)
	100	1.09±0.011(1.11)	8.1±0.575(8.71)	38.44±0.722(39.1)	3.44±0.23(3.6)
	120	1.03±0.051(1.04)	10.1±0.585(10.6)	54.02±3.44(57.4)	5.54±0.85(6.4)
	140	0.95±0.057(1.01)	9.2±0.307(9.59)	49.14±4.751(53.8)	4.36±0.54(4.9)
	160	0.90±0.086(0.98)	9.4±0.346(9.83)	44.51±1.749(46.2)	3.64±0.46(4.1)
PM6: BTSCN-	As-cast	1.11±0.041(1.16)	2.6±0.273(2.88)	33.93±1.01(34.94)	1.05±0.121(1.1)

IDT, Chlorobenzene	100	0.92±0.089(1.01)	2.5±0.226(2.80)	30.89±0.86(31.75)	0.72±0.091(0.8)
	120	0.84±0.177(1.02)	2.9±0.35(3.27)	31.32±2.11(33.43)	0.87±0.202(1.0)
	140	0.64±0.22(0.86)	3.1±0.44(3.6)	29.01±1.41(30.42)	0.62±0.236(0.8)
	160	0.88±0.119(1.00)	3.4±0.266(3.74)	31.44±1.07(32.51)	1.04±0.205(1.2)
PM6: BTSCN- IDT, Chloroform	As-cast	1.12±0.019(1.14)	3.4±0.07(3.53)	32.79±0.50(33.29)	1.26±0.036(1.3)
	100	1.12±0.013(1.14)	4.4±0.257(4.75)	36.84±0.467(37.31)	1.86±0.11(1.9)
	120	1.07±0.047(1.12)	3.6±0.788(4.40)	39.03±2.01(41.04)	2.17±0.329(2.5)
	140	1.01±0.012(1.03)	7.0±0.770(7.80)	44.82±2.47(47.79)	3.18±0.490(3.6)
	160	1.02±0.018(1.04)	6.2±0.420(6.65)	40.80±0.66(41.46)	2.72±0.248(2.9)

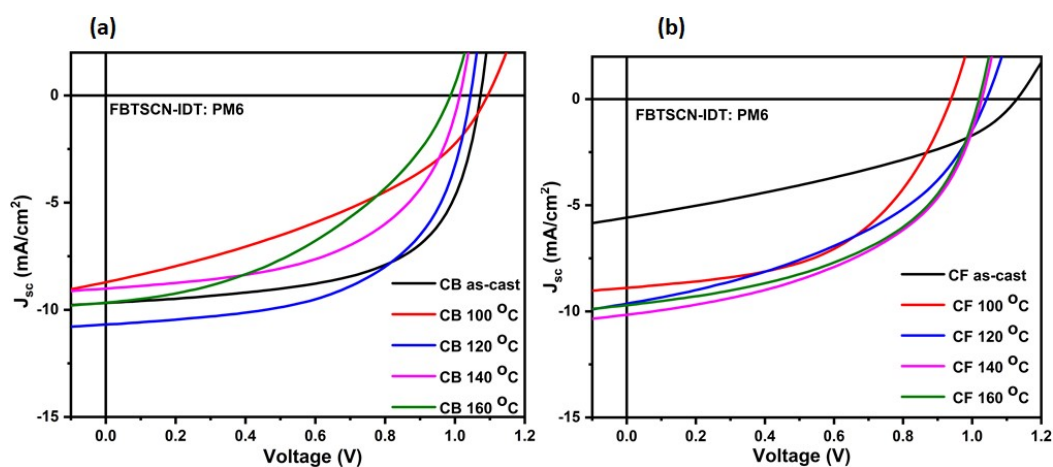


Figure S28. J-V characteristics of FBTSCN-IDT: PM6 blend system of (a) chlorobenzene, and (b) chloroform-based devices, under 1 Sun.

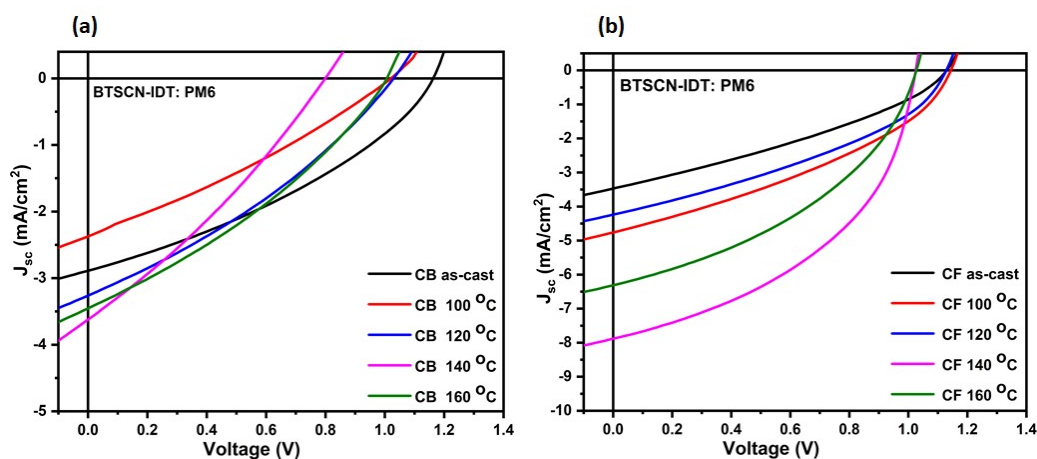


Figure S29. J-V characteristics of BTSCN-IDT: PM6 blend system of (a) chlorobenzene, and (b) chloroform-based devices, under 1 Sun.

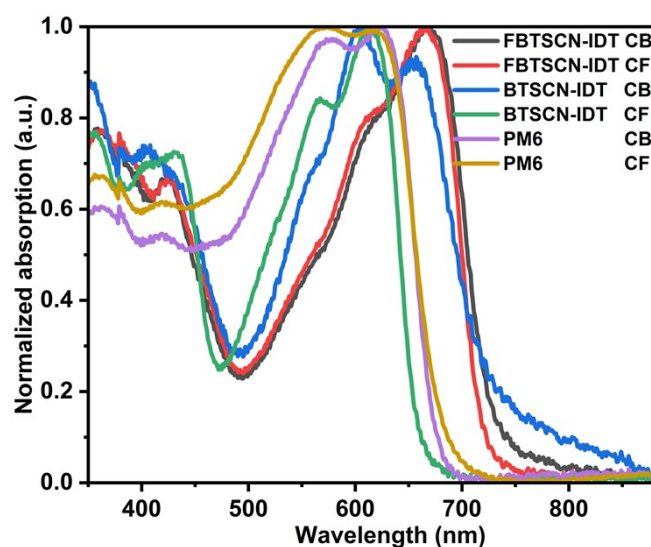


Figure S30. The normalized absorption spectra of pristine FBTSCN-IDT, BTSCN-IDT, and PM6 molecule thin films in chlorobenzene and chloroform solvents.

Charge carrier mobility:

Table S3. The photoactive layer film thickness and values of β obtained from SCLC fitting for hole and electron only devices.

Sample	Thickness (nm)	Electron/Hole mobility ($\text{cm}^2/\text{v.s}$)	β (V/cm) ⁻¹
Hole only devices			
FBTSCN-IDT: PM6 CB	628.2	1.82×10^{-4}	0.00488
FBTSCN-IDT: PM6 CF	1386.8	2.71×10^{-4}	0.00263
BTSCN-IDT: PM6 CB	1499.0	1.72×10^{-5}	0.00127
BTSCN-IDT: PM6 CF	686.4	2.02×10^{-4}	0.00032
Electron only devices			
FBTSCN-IDT: PM6 CB	628.2	1.51×10^{-6}	0.000340
FBTSCN-IDT: PM6 CF	1386.8	4.36×10^{-6}	0.000044
BTSCN-IDT: PM6 CB	1499.0	1.99×10^{-7}	0.001500
BTSCNO-IDT: PM6 CF	686.4	2.32×10^{-7}	0.002510

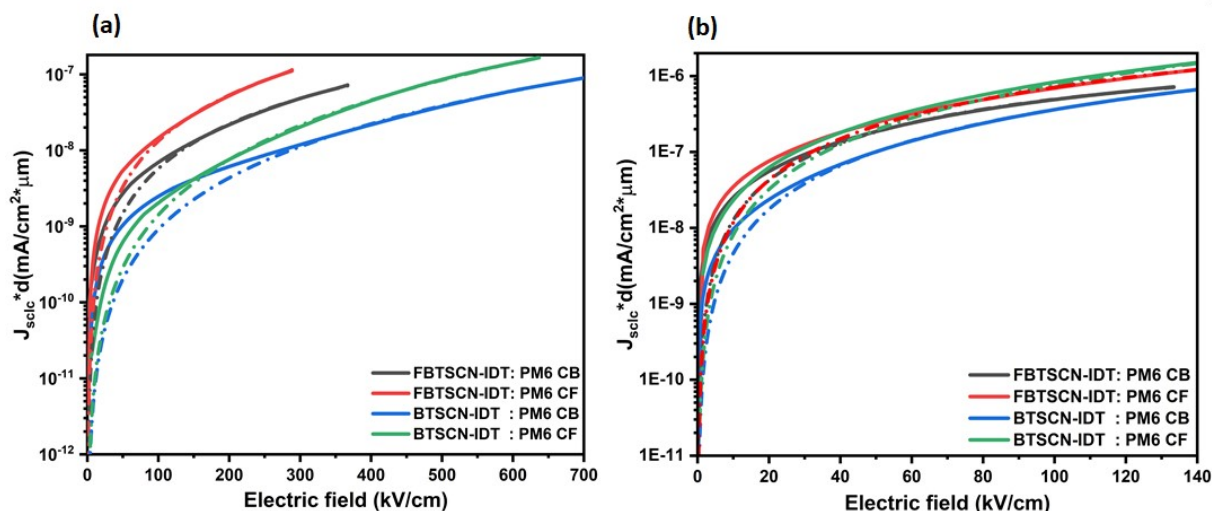


Figure S31. Charge carrier transport data of FBTSCN-IDT/BTSCN-IDT: PM6 devices of hole and electron configuration with SCLC fittings (dotted lines), (a) electron only configuration of ITO/ZnO/active layer/Ca/Al, and (b) hole only configuration of ITO/PEDOT:PSS/Active layer/MoO₃/Ag device structures.

Indoor performance:

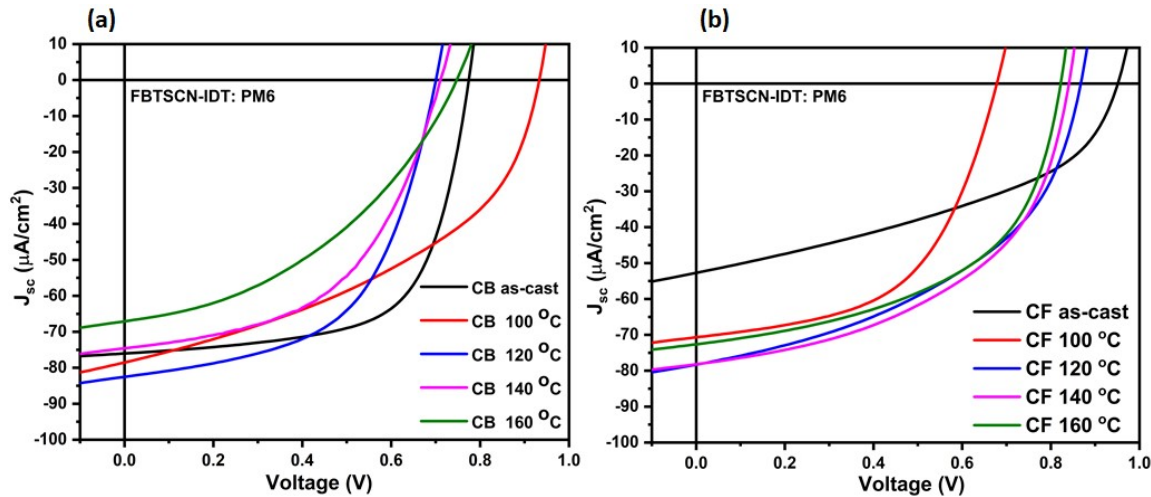


Figure S32. J-V characteristics of FBTSCN-IDT: PM6 blend system of (a) chlorobenzene, and (b) chloroform-based devices, under 1000 lux (fluorescent lamp, 2700K).

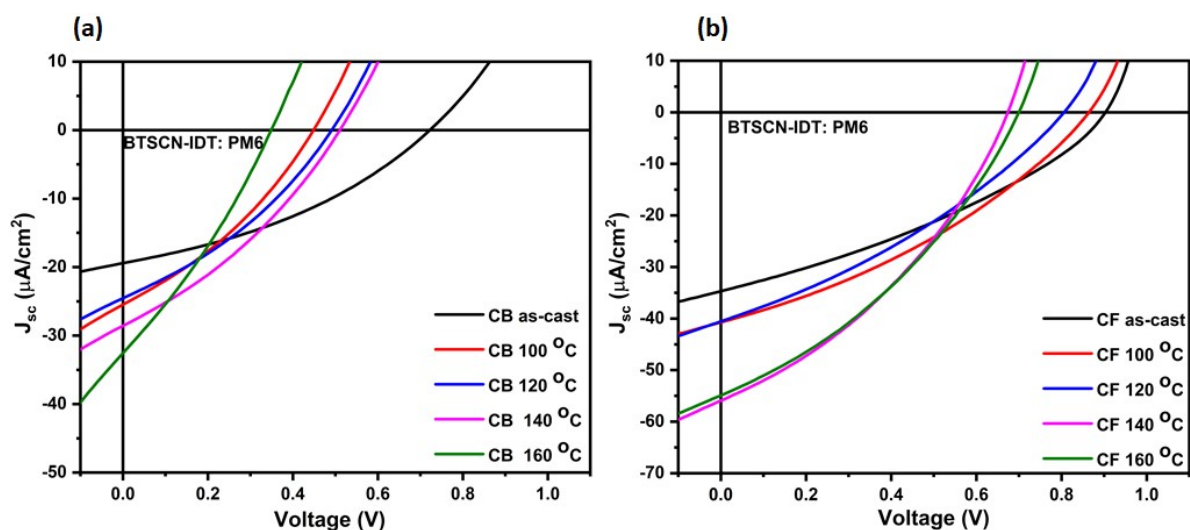


Figure S33. J-V characteristics of BTSCN-IDT: PM6 blend system of (a) chlorobenzene, and (b) chloroform-based devices, under 1000 lux (fluorescent lamp, 2700K).

Table S4. Summary of photovoltaic performance of FBTSCN-IDT/BTSCN-IDT: PM6 photoactive layer-based device measurement under fluorescent lamp (1000 lux).

Active Layer	Thermal annealing (°C)	V_{oc} (V)	J_{sc} ($\mu\text{A}/\text{cm}^2$)	FF (%)	O/P Power ($\mu\text{W}/\text{cm}^2$)
PM6: FBTSCN-IDT, Chlorobenzene	As-cast	0.70±0.069(0.77)	73.8±0.005(73.9)	59.5±6.65(66.15)	35.1±3.30(38.2)
	100	0.88±0.053(0.93)	78.4±0.004(78.5)	35.81±7.66(43.47)	25.9±5.82 (31.8)
	120	0.65±0.044(0.70)	82.4±0.008(82.5)	49.98±6.43(56.41)	26.9±3.84 (30.74)
	140	0.64±0.074(0.71)	72.1±0.005(72.2)	50.57±5.10(55.67)	23.97±3.33 (27.3)
	160	0.58±0.151(0.74)	75.2±0.005(75.3)	43.68±3.07(46.75)	18.1±2.5 (20.6)
PM6: FBTSCN-IDT, Chloroform	As-cast	0.93±0.016(0.95)	52.6±0.001(52.7)	41.1±0.55(41.65)	19.6±1.3(20.9)
	100	0.58±0.088(0.67)	70.1±0.031(70.22)	53.91±1.99(55.9)	26.4±6.5(32.9)
	120	0.82±0.040(0.86)	78.2±0.007(78.3)	40.45±5.70(46.15)	25.1±6.2(31.3)
	140	0.83±0.008(0.84)	78.1±0.001(78.2)	47.77±2.09(49.86)	30.6±2.3(32.9)
	160	0.80±0.020(0.82)	74.4±0.001(74.5)	50.37±2.02(52.39)	29.29±2.01(31.3)
PM6: BTSCN-IDT, Chlorobenzene	As-cast	0.60±0.112(0.72)	24.1±0.002(24.12)	33.3±2.718(36.08)	3.92±1.15(5.07)
	100	0.40±0.040(0.44)	25.4±0.001(25.5)	31.68±1.30(32.99)	3.1±0.6(3.7)
	120	0.41±0.072(0.49)	35.8±0.001(35.9)	34.20±1.32(35.57)	3.3±0.7 (4.0)
	140	0.40±0.104(0.51)	30.3±0.002(30.4)	30.98±1.87(32.85)	3.4±1.4(4.80)
	160	0.28±0.060(0.34)	32.8±0.0002(32.9)	28.83±1.05(29.88)	2.75±0.65(3.4)
PM6: BTSCN-IDT, Chloroform	As-cast	0.82±0.080(0.90)	36.6±0.002(34.7)	32.25±1.51(33.76)	8.9±1.7(10.6)
	100	0.79±0.066(0.86)	42.3±0.002(42.4)	33.31±1.09(34.4)	11.41±0.72(12.1)
	120	0.78±0.044(0.83)	40.5±0.003(40.6)	36.25±2.19(38.44)	9.81±1.03(10.8)

	140	0.64±0.052(0.70)	59.6±0.005(59.7)	34.2±1.481(35.7)	12.47±1.01(13.4)
	160	0.69±0.035(0.73)	54.8±0.004(54.9)	37.12±1.81(38.93)	12.85±0.81 (13.6)